Advances in Computational Mathematics (2006) 24: 81–112

Quadratic immersed finite element spaces and their approximation capabilities

Brian Camp [a], Tao Lin [a], Yanping Lin [b,⋆] and Weiwei Sun [c,⋆⋆]

[a] *Department of Mathematics, Virginia Tech, USA*
[b] *Department of Mathematics Sciences, University of Alberta, Canada and Northeastern University at Qinhuangdao, Qinhuangdao, Hebei, China*
[c] *Department of Mathematics, City University of Hong Kong, Hong Kong, China*

Received 9 November 2003; accepted 21 June 2004
Communicated by Yuesheng Xu

Dedicated to the 60th birthday of Charles A. Micchelli

This paper discusses a class of quadratic immersed finite element (IFE) spaces developed for solving second order elliptic interface problems. Unlike the linear IFE basis functions, the quadratic IFE local nodal basis functions cannot be uniquely defined by nodal values and interface jump conditions. Three types of one dimensional quadratic IFE basis functions are presented together with their extensions for forming the two dimensional IFE spaces based on rectangular partitions. Approximation capabilities of these IFE spaces are discussed. Finite element solutions based on these IFE for representative interface problems are presented to further illustrate capabilities of these IFE spaces.

Keywords: interface problem, discontinuous coefficients, structured mesh, quadratic immersed finite element methods, order of convergence, error bounds.

Mathematics subject classifications (2000): 65N15, 65N30, 65N50, 65Z05.

1. Introduction

The main purpose of this paper is to present a class of quadratic immersed finite element (IFE) spaces developed for solving the following second-order elliptic interface problems whose coefficients are piecewise-constant functions: in a domain $\Omega \subset \mathbb{R}^n$ ($n = 1$ or 2), find the function u such that

$$-\nabla \cdot \big(p(\mathbf{x})\nabla u(\mathbf{x})\big) = f(\mathbf{x}), \quad \mathbf{x} \in \Omega, \tag{1.1}$$

⋆ Supported by NSERC.
⋆⋆ This work was supported in part by a grant from the Research Grants Council of the Hong Kong Special Administrative Region, China (project CityU 1141/01P).

with a certain boundary condition, say a Dirichlet boundary condition

$$u|_{\partial\Omega} = g, \tag{1.2}$$

and following jump conditions across an interface $\Gamma \subset \Omega$:

$$[u]|_\Gamma = 0, \tag{1.3}$$

$$[p\mathbf{n} \cdot \nabla u]|_\Gamma = 0. \tag{1.4}$$

Here, for the simplicity of presentation, the domain Ω, either an interval (in the one dimensional case) or a rectangle (in the two dimensional case), is assumed to be split into two separate regions Ω_1 and Ω_2 by an interface Γ so that $\Omega = \Omega_1 \cup \Omega_2 \cup \Gamma$, see figure 1. The coefficient $p(\mathbf{x})$ is a piecewise constant function defined according to the interface Γ

$$p(\mathbf{x}) = \begin{cases} p_1, & \mathbf{x} \in \Omega_1, \\ p_2, & \mathbf{x} \in \Omega_2. \end{cases} \tag{1.5}$$

The notation $[u](\mathbf{x})$ stands for the jump of $u(\mathbf{x})$ across the interface Γ with the following understanding: for any point $\mathbf{x}$ on the interface Γ,

$$[u](\mathbf{x}) = \lim_{\mathbf{y}\to\mathbf{x},\mathbf{y}\in\Omega_1} u(\mathbf{y}) - \lim_{\mathbf{z}\to\mathbf{x},\mathbf{z}\in\Omega_2} u(\mathbf{z}).$$

The same definition applies to the scalar function $p\ \mathbf{n} \cdot \nabla u(\mathbf{x})$.

It is well known that efficiently solving interface problems of this type is critical for numerical simulations in many applications of engineering and sciences. Many approaches have been taken for solving the interface problem (1.1)–(1.4). For example, finite difference (FD) methods [11,23,24], finite element (FE) method [1], and collocation methods [22] have been developed to solve interface problems. Both finite difference and finite element methods can yield satisfactory numerical results in many applications. For example, it is well known (see [5,7] and the references therein) that the standard Galerkin method with linear finite elements can be used to solve such elliptic interface problems with the optimal $O(h^2)$ accuracy in the numerical solutions so long as the triangles in the partition are aligned with the interface, i.e., the interface is allowed to pass a triangle

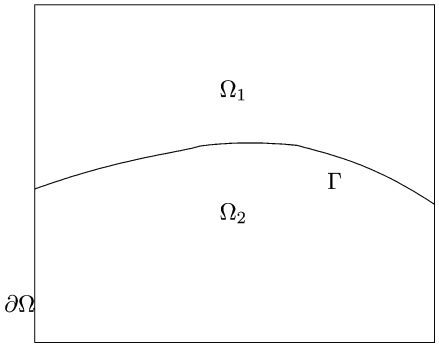

Figure 1. The domain Ω with an interface Γ.

only through two of its vertices. One of the drawbacks of the finite difference approach is its lack of versatility for handling the arbitrary variations of the interface curve, even though many remedies have been developed, see for example [9,12,14,20,21].

Article [2] introduces a class of generalized finite element framework intended to handle boundary value problems with rough coefficients including interface problems. The basic idea of this generalized finite element framework is to design suitable finite element spaces by modifying a standard finite element space according to a particular problem under consideration. In particular, jump conditions are required in the construction of the finite element spaces for an interface problem. The immersed finite element (IFE) methods [10,15–18] for interface problems can be considered as specific implementations of this general idea. For example, the implementation of this framework with linear polynomials for the one-dimensional interface problem coincides with the one dimensional IFE method [15], and the two-dimensional implementation with linear polynomials in [3] is only slightly different from the IFE method discussed in [16,17]. However, how to satisfactorily implement this general framework with higher degree polynomials for interface problems is still open for investigation. There are many ways to realize this general idea with higher degree polynomials, and a particular implementation of this general idea is not necessarily the optimal from the point of view of the accuracy expected from the higher-degree polynomials employed [2].

The central idea of immersed finite elements is to use a partition $\mathcal{T}_h$ independent of the interface Γ so that partitions with simple and efficient structures, such as a Cartesian partition, can be used to satisfactorily solve an interface problem with a rather complicated or varying interface. A partition used in an IFE method consists of two types of elements: interface elements which are cut through by interface Γ and the rest are non-interface elements. Then the standard FE basis functions are used in each of the non-interface elements. However, in an interface element, the local nodal basis functions are constructed with polynomials piece-wisely defined according to the interface such that these functions can satisfy the jump conditions (either exactly or approximately) across the interface and retain specified values at the nodes of this interface element. These local nodal basis functions are also required to have the H^1 regularity such that they can be used to construct IFE spaces for solving the interface problems. The idea is used in [3] and is similar to that used for the Hsieh–Clough–Tocher macro C^1 element [4] where each basis function consists of three cubic polynomials on the subtriangles formed by connecting the vertices and the center of gravity so that the required continuity can be satisfied. In summary, the following are the two major differences between the IFE methods and the standard FE methods for interface problems:

- To maintain the accuracy, the partition used in the standard FE method has to be formed according to the interface Γ while the partition of an IFE method can be formed independently of the interface.
- On the other hand, the basis functions in the standard FE method are formed independent of the interface while some of the basis functions in the IFE method will incorporate the interface location and the interface jump conditions.

The IFE methods are therefore preferable alternatives for those applications, see for example [8], in which an interface problem has to be solved repeatedly, each time with a different interface Γ (either due to variation in its shape or the position), and for many applications that may also prevent the usage of the standard finite element method because of the involved nontrivial interfaces, see for example [19] and references therein.

This paper aims to continue the development of the general framework of [2] via IFE methods. There have been publications about IFE spaces using linear [3,15–17] and bilinear [18] polynomials. The natural next step is to study the IFE spaces based on quadratic polynomials because of both the academic and computational reasons. We intend to explore how to develop quadratic IFE spaces with optimal approximation capability which, to our best knowledge, has not been addressed in literature. Since different implementation ideas are employed, the IFE spaces presented here are therefore not in the same class as those in [2]. Compared to the quadratic implementation in [2], the approximation capability of these quadratic IFE spaces are of higher order, and they are closely related to the standard quadratic FE space in the sense that they reduce to the standard quadratic FE space when the discontinuity in the coefficient disappears or when the discontinuity happens on the edges of the elements in the partition. Computationally, a higher degree IFE space is often more efficient than its counterparts using polynomials with a lower degree. In a typical numerical simulation with a specific error tolerance $\text{tol} > 0$, the method with polynomials of a higher degree may generate a satisfactory numerical result with a coarser partition which in turn involves an algebraic system with fewer unknowns than the corresponding lower degree methods.

This paper is organized as follows. In Section 2, three types of one-dimensional quadratic IFE spaces will be introduced. The first one is without any extra condition explicitly imposed while each of the other two has one extra condition. We will then further extend these spaces to two dimensions to form corresponding biquadratic IFE spaces. In section 3, numerical experiments will be presented to investigate the interpolation approximation capabilities of these IFE spaces. Finite element solutions based on these IFE spaces for typical interface problems will also be presented. We would also like to point out that even though only homogeneous interface jump conditions are considered here, the IFE spaces developed in this paper can also be used to handle those interface problems with nonhomogeneous jump conditions through the usual homogenization procedures.

2. Quadratic immersed finite element spaces

In this section, we will discuss three types of quadratic IFE spaces whose local nodal basis functions are: (1) hierarchical basis functions formed as products of the linear IFE basis fuctions, with no extra condition explicitly imposed on the interface; (2) basis functions with one extra continuity requirement across the interface; (3) basis functions which use a form of local refinement around the interface. Each of these basis functions is discussed in detail in sections 2.1 and 2.2 below. As we can see later, there are infinitely many ways to define the quadratic IFE nodal basis functions

that can satisfy the nodal value specification and interface jump conditions. The three IFE spaces presented here demonstrate what will happen if no extra condition is imposed and how to add extra conditions suitably. In addition, we will show that these IFE spaces possess many important properties similar to those of the standard FE spaces, such as the partition of unity, and two of these IFE spaces even become the standard quadratic FE space when the interface curve coincides with a line used in the partition or when the coefficient function has no discontinuity.

2.1. *Quadratic immersed finite element spaces in one dimension*

We start the discussion by considering one-dimensional quadratic IFE spaces. To facilitate the discussion, we first introduce notations used in this and later sections.

In one dimension, we let Ω be the typical interval $(0, 1)$, and the interface Γ consists of just one point at $x = \alpha \in (0, 1)$. The interface problem (1.1)–(1.4) then becomes

$$-\big(p(x)u'(x)\big)' = f(x), \quad x \in \Omega = (0, 1), \tag{2.1}$$

$$u(0) = g_0 \quad \text{and} \quad u(1) = g_1, \tag{2.2}$$

$$u(\alpha-) = u(\alpha+), \tag{2.3}$$

$$p_1 u'(\alpha-) = p_2 u'(\alpha+). \tag{2.4}$$

Here, the coefficient p is defined by

$$p(x) = \begin{cases} p_1, & x < \alpha, \\ p_2, & x \geqslant \alpha, \end{cases} \tag{2.5}$$

with two positive constants p_1 and p_2. All the discussions here can be readily extended to the case in which the interface Γ consists of multiple interface points and the coefficient function $p(x)$ is formed by multiple constant functions.

Let $\mathcal{T}_h = \bigcup_{k=1}^{n} e_k$ be a partition of $\overline{\Omega} = [0, 1]$, where elements $e_k = [x_{2(k-1)}, x_{2k}]$ are intervals in Ω formed by node points

$$0 = x_0 < x_1 < x_2 < x_3 < x_4 < \cdots < x_{2n-1} < x_{2n} = 1,$$

such that

$$x_{2k-1} = \frac{x_{2k} + x_{2k-2}}{2}, \quad k = 1, 2, \ldots, n.$$

Without loss of generality, we consider a uniform partition such that $x_{2k} = x_0 + kh$ where $x_0 = 0$ (the left endpoint of Ω) and $h = 1/n$. The local quadratic nodes on the kth element e_k will be denoted by $t_{k,1} = x_{2(k-1)}$, $t_{k,2} = x_{2k-1}$ and $t_{k,3} = x_{2k}$.

We categorize all the elements into two classes as follows.

Definition 2.1. An element e_k of the partition $\mathcal{T}_h$ is called an *interface element* if the interface point α is in the interior of e_k, i.e., $x_{2(k-1)} < \alpha < x_{2k}$. Any element which is not an interface element will be called a *noninterface element*.

If the kth element e_k is a noninterface element, then we use the three standard Lagrange type quadratic FE local nodal functions $\phi_{k,i}(x)$, $i = 1, 2, 3$, such that

$$\phi_{k,i}(t_{k,j}) = \begin{cases} 1, & \text{if } i = j, \\ 0, & \text{if } i \neq j, \end{cases} \quad j = 1, 2, 3. \tag{2.6}$$

The formulae for the standard local nodal nodal basis functions $\phi_{k,i}(x)$, $i = 1, 2, 3$, are easy to derive since each one is the unique quadratic Lagrange interpolant of the nodal values given in (2.6).

In the next three subsections, we will give three different approaches for constructing local nodal basis functions $\phi_{k,i}(x)$, $i = 1, 2, 3$, in an interface element e_k that can satisfy the same nodal value specifications (2.6) and interface jump conditions (2.3) and (2.4). Then for each node x_i, $i = 0, 1, \ldots, 2n$, we will use these local basis functions to form a global Lagrange type basis function, and our IFE spaces are defined as the linear spaces spanned by these basis functions.

2.1.1. A one-dimensional hierarchical quadratic IFE space

Following the same idea used for local nodal basis functions of the standard quadratic FE space, see [6,13] for example, we will demonstrate that the quadratic IFE local nodal basis functions in an interface element e_k can be constructed hierarchically by multiplying together two linear IFE interpolation functions (to be defined in the next paragraph) which are a generalization of the linear IFE local nodal basis functions [15]. This approach can yield quadratic IFE spaces without using any extra conditions and the idea can be repeatedly used to generate IFE spaces of degree three, and so on.

First, we modify the linear IFE local nodal basis functions [15] such that its nodal values can be specified at two points that may or may not be on both sides of the interface point. Specifically, for each pair of indices (i, j) with $i = 1, 2, 3$, $j = 1, 2, 3$ but $i \neq j$, we form a linear IFE interpolation function that is a piecewise linear function of the following form

$$l_{i,j}(x) = \begin{cases} a_1 x + a_0, & \text{if } x < \alpha, \\ b_1 x + b_0, & \text{if } x \geqslant \alpha, \end{cases} \tag{2.7}$$

whose coefficients a_0, a_1, b_0, b_1 are chosen such that $l_{i,j}(x)$ can satisfy the nodal value specification and interface jump conditions as follows:

$$\begin{aligned} &l_{i,j}(t_{k,i}) = 1, \quad l_{i,j}(t_{k,j}) = 0 \qquad \text{(nodal value specification)}, \\ &[l_{i,j}]_{x=\alpha} = 0, \quad \left[p l'_{i,j}\right]_{x=\alpha} = 0 \quad \text{(interface jump conditions)}. \end{aligned} \tag{2.8}$$

Theorem 2.1. The linear immersed interpolating function $l_{i,j}(x)$ $(i \neq j)$ is uniquely determined.

Proof. When α is not in the interval formed by $t_{k,i}$ and $t_{k,j}$, say $t_{k,i} < t_{k,j}$ and $\alpha < t_{k,i}$, then (2.8) leads to the following linear system about the coefficients a_0, a_1, b_0 and b_1:

$$\begin{pmatrix} 0 & 0 & t_{k,i} & 1 \\ 0 & 0 & t_{k,j} & 1 \\ \alpha & 1 & -\alpha & -1 \\ p_1 & 0 & -p_2 & 0 \end{pmatrix} \begin{pmatrix} a_1 \\ a_0 \\ b_1 \\ b_0 \end{pmatrix} = \begin{pmatrix} 1 \\ 0 \\ 0 \\ 0 \end{pmatrix}. \tag{2.9}$$

Since the determinant of coefficient matrix in (2.9) is $-p_1(t_{k,i} - t_{k,j})$ which is always non-zero, (2.9) will always have a unique solution. Similar arguments apply to the situations where $t_{k,i} < \alpha < t_{k,j}$ and $t_{k,i} < t_{k,j} < \alpha$. Hence the linear IFE interpolation functions are uniquely determined. □

Note that the proof of theorem 2.1 provides a procedure to form $l_{i,j}(x)$. The following lemma shows that $l_{j,i}(x)$ (where $i < j$) and $l_{i,j}(x)$ are related.

Lemma 2.1. The linear immersed interpolating functions $l_{i,j}(x)$ and $l_{j,i}(x)$ (where $i < j$) are related by $l_{j,i}(x) = 1 - l_{i,j}(x)$ for all values of x.

Proof. We need to show that $l_{i,j}(x) + l_{j,i}(x) \equiv 1$ where $l_{i,j}(x)$ has the general form

$$l_{i,j}(x) = \begin{cases} a_1 x + a_0, & \text{if } x < \alpha, \\ b_0 x + b_0, & \text{if } x \geqslant \alpha, \end{cases} \tag{2.10}$$

and $l_{j,i}(x)$ has the general form

$$l_{j,i}(x) = \begin{cases} \tilde{a}_1 x + \tilde{a}_0, & \text{if } x < \alpha, \\ \tilde{b}_0 x + \tilde{b}_0, & \text{if } x \geqslant \alpha. \end{cases} \tag{2.11}$$

Let $\alpha < t_{k,i}$. Then the function $f(x)$ which is defined by $f(x) = l_{i,j}(x) + l_{j,i}(x)$ will have the general form

$$f(x) = \begin{cases} (a_1 + \tilde{a}_1)x + (a_0 + \tilde{a}_0), & \text{if } x < \alpha, \\ \big(b_0 + \tilde{b}_0\big)x + \big(b_0 + \tilde{b}_0\big), & \text{if } x \geqslant \alpha. \end{cases} \tag{2.12}$$

Since both $l_{i,j}(x)$ and $l_{j,i}(x)$ satisfy the interface conditions (2.3) and (2.4) then $f(x)$ also satisfies the interface conditions. This leads to a linear system whose coefficient matrix is the same as that in (2.9). Hence, this system has a unique solution such that

$$a_1 + \tilde{a}_1 = b_1 + \tilde{b}_1 = 0 \tag{2.13}$$

and

$$a_0 + \tilde{a}_0 = b_0 + \tilde{b}_0 = 1. \tag{2.14}$$

Therefore, $f(x) \equiv 1$ and so $l_{j,i}(x) = 1 - l_{i,j}(x)$. Similar arguments hold in the cases where $t_{k,i} < \alpha < t_{k,j}$ or $t_{k,j} < \alpha$. □

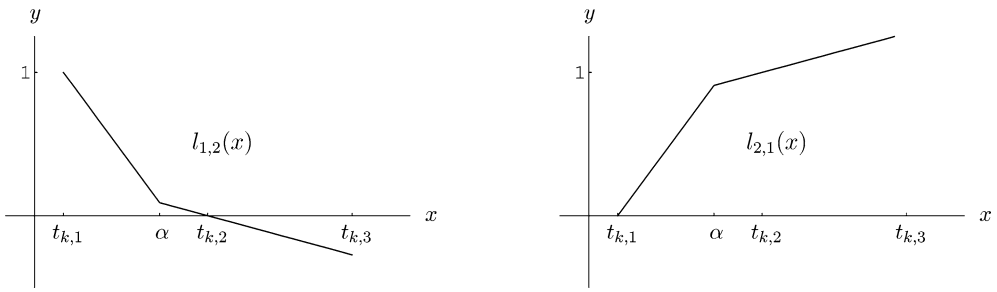

Figure 2. The linear immersed interpolating functions $l_{1,2}(x)$ and $l_{2,1}(x)$ on the element e_k.

Remark 2.1. The linear immersed interpolation functions $l_{1,3}(x)$ and $l_{3,1}(x)$ are the usual linear IFE local nodal basis functions [15] on the interface element e_k. Consequently, the above discussion has shown that linear IFE local nodal basis functions are unique and that they satisfy a partition of unity since $l_{1,3}(x) + l_{3,1}(x) \equiv 1$.

The immersed linear interpolation functions $l_{1,2}(x)$ and $l_{2,1}(x)$ on the element e_k can be seen in figure 2 for the case where $t_{k,1} < \alpha < t_{k,2}$. The plots of $l_{1,3}(x)$, $l_{3,1}(x)$, $l_{2,3}(x)$ and $l_{3,2}(x)$ are similar although they are omitted here due to space limitations.

Now we can define the three quadratic local nodal IFE basis functions as follows:

$$\widetilde{\phi}_{k,1}(x) = l_{1,2}(x)l_{1,3}(x), \quad \widetilde{\phi}_{k,2}(x) = l_{2,1}(x)l_{2,3}(x), \quad \widetilde{\phi}_{k,3}(x) = l_{3,1}(x)l_{3,2}(x). \quad (2.15)$$

First, it can be easily verified that these functions satisfy the nodal value specification $i = 1, 2, 3$,

$$\widetilde{\phi}_{k,i}(t_{k,j}) = \begin{cases} 1, & \text{if } i = j, \\ 0, & \text{if } i \neq j, \end{cases} \qquad j = 1, 2, 3.$$

The following theorem states some important properties of these functions including satisfying the interface jump conditions (2.3) and (2.4). The proof of this theorem is a matter of straightforward verifications, and is therefore omitted.

Theorem 2.2. The quadratic local nodal IFE basis functions $\widetilde{\phi}_{k,i}(x), i = 1, 2, 3$, in (2.15) have the following properties:

1. They satisfy the interface jump conditions (2.3) and (2.4).
2. $\sum_{i=1}^{3} \widetilde{\phi}_{k,i}(x) \equiv 1$ for all $x \in e_k$.
3. These local nodal IFE basis functions $\widetilde{\phi}_{k,i}(x),\ i = 1, 2, 3$, are consistent with the standard local nodal FE basis functions $\phi_{k,i}(x),\ i = 1, 2, 3$, in the following sense:
   (a) $\lim_{\alpha \to t_{k,1}} \widetilde{\phi}_{k,i}(x) = \phi_{k,i}(x)$ and $\lim_{\alpha \to t_{k,3}} \widetilde{\phi}_{k,i}(x) = \phi_{k,i}(x)$ for $i = 1, 2, 3$.
   (b) If $p_1 = p_2 > 0$ then $\widetilde{\phi}_{k,i}(x) = \phi_{k,i}(x)$.

We now proceed to construct an IFE space using these local nodal basis functions. First, for each element $e_k \in \mathcal{T}_h$, we let

$$\widetilde{S}_h(e_k) = \begin{cases} span\{\phi_{k,i}(x),\ i = 1, 2, 3\}, & \text{if } e_k \text{ is a noninterface element,} \\ span\{\widetilde{\phi}_{k,i}(x),\ i = 1, 2, 3\}, & \text{if } e_k \text{ is an interface element.} \end{cases}$$

Then, for each node $x_i,\ i = 1, 2, \ldots, 2n$, we let $\widetilde{\phi}_i(x)$ be a piecewise quadratic polynomial such that $\widetilde{\phi}_i|_{e_k} \in \widetilde{S}_h(e_k)$ for any $e_k \in \mathcal{T}_h$, and

$$\widetilde{\phi}_i(x_j) = \begin{cases} 1, & \text{if } i = j, \\ 0, & \text{if } i \neq j. \end{cases}$$

Finally, we can form the IFE space over the whole domain by the hierarchical local nodal basis functions as follows:

$$\widetilde{S}_h(\Omega) = span\{\widetilde{\phi}_i,\ i = 0, 1, \ldots, 2n\}.$$

2.1.2. A one-dimensional quadratic IFE space with extra continuity

The approach presented in the previous section is not the only way to construct quadratic local nodal IFE basis functions. In this section, following a similar idea presented in [15–17], we will form the quadratic local nodal IFE basis functions directly from piecewise quadratic polynomials using an undetermined coefficient technique.

In a typical interface element e_k, the interface point α separates e_k into two subintervals. We can use two quadratic polynomials defined on each of these subintervals to form a quadratic local nodal IFE basis function with the following form:

$$\overline{\phi}_{k,i}(x) = \begin{cases} a_2x^2 + a_1x + a_0, & \text{if } x < \alpha, \\ b_2x^2 + b_1x + b_0, & \text{if } x \geqslant \alpha. \end{cases} \tag{2.16}$$

Here, as usual, we need to choose the coefficients a_2, a_1, a_0, b_2, b_1 and b_0 such that the following conditions are satisfied:

$$\begin{cases} \overline{\phi}_{k,i}(t_{k,j}) = \begin{cases} 1, & \text{if } i = j, \\ 0, & \text{if } i \neq j \end{cases} & \text{(nodal value specification),} \\ \left[\overline{\phi}_{k,i}\right]_{x=\alpha} = 0, \quad \left[p\overline{\phi}'_{k,i}\right]_{x=\alpha} = 0 & \text{(interface jump conditions).} \end{cases} \tag{2.17}$$

However, (2.17) supplies only five conditions while $\overline{\phi}_{k,i}(x)$ contains six coefficients to be determined so one extra condition needs to be added.

Although any arbitrary condition may be used to provide a sixth condition, a natural condition to impose is another continuity requirement at the interface. By definition, we know that the solution $u(x)$ to the one dimensional interface problem (2.1)–(2.4) and its flux $p(x)u'(x)$ are both continuous at the interface. Moreover, it often happens that $(p(x)u'(x))'$ is continuous at the interface as well. For example, this is true when the right-hand side function $f(x)$ in (2.1) is continuous over Ω. This leads to one extra

condition at the interface that requires the local nodal IFE basis functions to satisfy the following:

$$\left[\left(p\overline{\phi}'_{k,i}\right)'\right]_{x=\alpha} = 0, \quad i = 1, 2, 3. \tag{2.18}$$

Quadratic local nodal IFE basis functions that are constructed using (2.18) as an extra continuity requirement will be referred to with the notation $\overline{\phi}_{k,i}$ in order to distinguish them from the other quadratic IFE local basis functions.

Theorem 2.3. The quadratic local nodal IFE basis functions, $\overline{\phi}_{k,i}(x)$, $i = 1, 2, 3$, are uniquely determined on an element e_k.

Proof. Without loss of generality, we assume that $\beta = p_2/p_1 > 1$. Consider the quadratic local nodal IFE basis function $\overline{\phi}_{k,1}(x)$. If $t_{k,1} < \alpha < t_{k,2}$ then the coefficients in (2.16) will satisfy the following system of equations:

$$\begin{pmatrix} t_{k,1}^2 & t_{k,1} & 1 & 0 & 0 & 0 \\ 0 & 0 & 0 & t_{k,2}^2 & t_{k,2} & 1 \\ 0 & 0 & 0 & t_{k,3}^2 & t_{k,3} & 1 \\ \alpha^2 & \alpha & 1 & -\alpha^2 & -\alpha & -1 \\ 2p_1\alpha & p_1 & 0 & -2p_2\alpha & -p_2 & 0 \\ 2p_1 & 0 & 0 & -2p_2 & 0 & 0 \end{pmatrix} \begin{pmatrix} a_2 \\ a_1 \\ a_0 \\ b_2 \\ b_1 \\ b_0 \end{pmatrix} = \begin{pmatrix} 1 \\ 0 \\ 0 \\ 0 \\ 0 \\ 0 \end{pmatrix}. \tag{2.19}$$

The determinant of the coefficient matrix is

$$-\frac{1}{4}p_1 h\big(h^2 + (\beta - 1)\big(-2\alpha^2 + 3h(\alpha - t_{k,1}) - 2t_{k,1}^2 + 4\alpha t_{k,1}\big)\big),$$

which is nonzero for $t_{k,1} \leqslant \alpha < t_{k,2}$. Hence (2.19) must have a unique solution, and the coefficients of $\overline{\phi}_{k,1}(x)$ are uniquely determined. The coefficients of $\overline{\phi}_{k,1}(x)$ satisfy a similar system with a nonsingular coefficient matrix when $t_{k,2} \leqslant \alpha \leqslant t_{k,3}$. So the quadratic local nodal IFE basis function $\overline{\phi}_{k,1}(x)$ is uniquely determined on the element e_k for the two possible locations of the interface point α. Similar arguments can be applied to show that the quadratic local nodal IFE basis functions $\overline{\phi}_{k,2}(x)$ and $\overline{\phi}_{k,3}(x)$ are also uniquely determined. □

The proof of theorem 2.3 provides a procedure for constructing the quadratic IFE local basis functions $\overline{\phi}_{k,i}(x)$. By their definition, these local nodal IFE basis functions satisfy the interface jump conditions. In addition, they also have the important properties stated in the following theorem which can be proved by direct verifications.

Theorem 2.4. The quadratic local nodal IFE basis functions $\overline{\phi}_{k,i}(x)$, $i = 1, 2, 3$, defined by (2.17) and (2.18) have the same properties as those of $\widetilde{\phi}_i(x)$, $i = 1, 2, 3$, stated in theorem 2.2.

Now, we are ready to construct an IFE space by these local nodal basis functions. First, for each element $e_k \in \mathcal{T}_h$, we let

$$\overline{S}_h(e_k) = \begin{cases} \text{span}\{\phi_{k,i}(x), i = 1, 2, 3\}, & \text{if } e_k \text{ is a noninterface element,} \\ \text{span}\{\overline{\phi}_{k,i}(x), i = 1, 2, 3\}, & \text{if } e_k \text{ is an interface element.} \end{cases}$$

Then, for each node x_i, $i = 1, 2, \ldots, 2n$, we let $\overline{\phi}_i(x)$ be a piecewise quadratic polynomial such that $\overline{\phi}_i|_{e_k} \in \overline{S}_h(e_k)$ for any $e_k \in \mathcal{T}_h$, and

$$\overline{\phi}_i(x_j) = \begin{cases} 1, & \text{if } i = j, \\ 0, & \text{if } i \neq j. \end{cases}$$

Finally, we can form the IFE space over the whole domain by the local nodal basis functions with extra continuity condition as follows:

$$\overline{S}_h(\Omega) = span\{\overline{\phi}_i, i = 0, 1, \ldots, 2n\}.$$

2.1.3. A one-dimensional IFE space with local mesh refinement

Another way of constructing quadratic IFE basis functions is through a local grid refinement process. Note that each interface element e_k is separated into two subelements by the interface point α, $[t_{k,1}, \alpha]$ and $[\alpha, t_{k,3}]$. We then introduce three nodes in each of these subelements which correspond to their endpoints and the midpoints. For example, the left subelement has the three nodes $t_{k,1}$, $(t_{k,1} + \alpha)/2$ and α. The quadratic local nodal IFE basis functions (referred to as $\widehat{\phi}_{k,i}$) in the interface element e_k are defined as piecewise quadratic polynomials

$$\widehat{\phi}_{k,i} = \begin{cases} \widehat{\phi}^1_{k,i}(x), & x \in [t_{k,1}, \alpha], \\ \widehat{\phi}^2_{k,i}(x), & x \in [\alpha, t_{k,3}], \end{cases} \quad i = 1, 2, 3, 4,$$

such that they satisfy the following interpolation conditions and interface requirements:

$$\begin{array}{ll} \widehat{\phi}_{k,j}(\hat{t}_{k,i}) = 1, \quad \widehat{\phi}_{k,j}(\hat{t}_{k,j}) = 0 & \text{(nodal value specification),} \\ \left[\widehat{\phi}_{k,j}\right]_{x=\alpha} = 0, \quad \left[p\widehat{\phi}'_{k,j}\right]_{x=\alpha} = 0 & \text{(interface jump conditions),} \end{array} \quad j = 1, 2, 3, 4, \tag{2.20}$$

where $\hat{t}_{k,i}$ are the the nodes of the new subelements excepting those that occur at the interface: $\hat{t}_{k,1} = t_{k,1}$, $\hat{t}_{k,2} = (t_{k,1} + \alpha)/2$, $\hat{t}_{k,3} = (\alpha + t_{k,3})/2$ and $\hat{t}_{k,4} = t_{k,3}$.

Theorem 2.5. The quadratic local nodal IFE basis functions $\widehat{\phi}_{k,i}(x)$, $i = 1, 2, 3, 4$, defined by (2.20) are uniquely determined.

Proof. Let e_k be an interface element so that $t_{k,1} < \alpha < t_{k,3}$. Consider the quadratic IFE local basis function $\widehat{\phi}_{k,1}(x)$ which is a piecewise quadratic function as in (2.16).

Since $\widehat{\phi}_{k,1}(x)$ is required to satisfy (2.20), then the coefficients a_2, a_1, a_0, b_2, b_1, and b_0 must satisfy the following system of linear equations:

$$\begin{pmatrix} (\hat{t}_{k,1})^2 & \hat{t}_{k,1} & 1 & 0 & 0 & 0 \\ (\hat{t}_{k,2})^2 & \hat{t}_{k,2} & 1 & 0 & 0 & 0 \\ 0 & 0 & 0 & (\hat{t}_{k,3})^2 & \hat{t}_{k,3} & 1 \\ 0 & 0 & 0 & (\hat{t}_{k,4})^2 & \hat{t}_{k,4} & 1 \\ \alpha^2 & \alpha & 1 & -\alpha^2 & -\alpha & -1 \\ 2p_1\alpha & p_1 & 0 & -2p_2\alpha & -p_2 & 0 \end{pmatrix} \begin{pmatrix} a_2 \\ a_1 \\ a_0 \\ b_2 \\ b_1 \\ b_0 \end{pmatrix} = \begin{pmatrix} 1 \\ 0 \\ 0 \\ 0 \\ 0 \\ 0 \end{pmatrix}. \tag{2.21}$$

The determinant of the coefficient matrix is a function of the interface location given by

$$q(\alpha) = -\frac{3}{16}(\alpha - t_{k,1})^2(\alpha - t_{k,3})^2(R + p_2 t_{k,1} - p_1 t_{k,3}), \quad R = \alpha(p_1 - p_2). \tag{2.22}$$

Since $(R + p_2 t_{k,1} - p_1 t_{k,3}) \neq 0$ for $\alpha \in e_k$, we can see see that $q(\alpha) \neq 0$ for $t_{k,1} < \alpha < t_{k,3}$. The system of linear equations above must have a unique solution for $t_{k,1} < \alpha < t_{k,3}$, and so the coefficients of $\widehat{\phi}_{k,1}(x)$ are determined uniquely. Similar arguments can be applied to show that functions $\widehat{\phi}_{k,i}(x)$, $i = 2, 3, 4$, are also uniquely determined. □

Remark 2.2. The quadratic local nodal IFE basis functions $\widehat{\phi}_{k,i}(x)$ are not consistent with standard local nodal FE basis functions. This means that if $p_1 = p_2$ or the interface approaches the boundary of e_k (i.e. $\alpha \to t_{k,1}$ or $\alpha \to t_{k,3}$), then $\widehat{\phi}_{k,i}(x)$ do not transform into the standard local nodal FE basis functions $\phi_{k,i}(x)$. This is because of the way in which the interface element e_k is divided into subelements, and subsequently there are four local nodal basis functions $\widehat{\phi}_{k,i}(x)$, $i = 1, \ldots, 4$.

However, by definition, these local nodal basis functions do satisfy the interface jump conditions, and they also satisfy a partition of unity as stated in the following theorem.

Theorem 2.6. The quadratic local nodal IFE basis functions $\widehat{\phi}_{k,i}(x)$, $i = 1, 2, 3, 4$, introduced above have the following property:

$$\sum_{i=1}^{4} \widehat{\phi}_{k,i}(x) \equiv 1 \quad \text{for all } x \in e_k. \tag{2.23}$$

Proof. This result follows easily from an argument similar to that used for proving lemma 2.1. □

Now, we can construct an IFE space by these local basis functions. First, for each element $e_k \in \mathcal{T}_h$, we let

$$\widehat{S}_h(e_k) = \begin{cases} \text{span}\{\phi_{k,i}(x), i = 1, 2, 3\}, & \text{if } e_k \text{ is a noninterface element,} \\ \text{span}\{\widehat{\phi}_{k,i}(x), i = 1, 2, 3, 4\}, & \text{if } e_k \text{ is an interface element.} \end{cases}$$

Then, for each node $x_i, i = 1, 2, \ldots, 2n+1$, we let $\widehat{\phi}_i(x)$ be a piecewise quadratic polynomial such that $\widehat{\phi}_i|_{e_k} \in \widehat{S}_h(e_k)$ for any $e_k \in \mathcal{T}_h$, and

$$\widehat{\phi}_i(x_j) = \begin{cases} 1, & \text{if } i = j, \\ 0, & \text{if } i \neq j. \end{cases}$$

Finally, we can form an IFE space over the whole domain by the local nodal basis functions with extra continuity condition as follows:

$$\widehat{S}_h(\Omega) = span\big\{\widehat{\phi}_i, i = 0, 1, \ldots, 2n\big\}.$$

2.2. *Two-dimensional immersed quadratic basis functions*

In this section, we extend the one-dimensional quadratic IFE spaces based upon $\widetilde{\phi}_{k,i}(x)$, $\overline{\phi}_{k,i}(x)$ and $\widehat{\phi}_{k,i}(x)$, to two-dimensional biquadratic IFE spaces with rectangular partitions where the interface Γ is a line parallel to one of the coordinate axes. In this configuration, a local biquadratic IFE basis function in an interface element can be constructed by taking the product of a standard FE local nodal basis function and an IFE local nodal basis function.

Before constructing the IFE spaces, we first restate the model interface BVP in two dimensions. We let the domain of the BVP problem (1.1)–(1.4) be the typical unit square $\Omega = [0, 1] \times [0, 1]$. We assume that the interface Γ is a horizontal line at $y = \gamma$ such that Ω_1 and Ω_2 will be defined as

$$\Omega_1 = \Omega \cap \big\{(x, y) \mid y < \gamma\big\},$$
$$\Omega_2 = \Omega \cap \big\{(x, y) \mid y > \gamma\big\}.$$

It should be noted that the methods for constructing biquadratic IFE spaces represented here can handle more general linear interfaces. For instance, the biquadratic IFE spaces in this section will be able to handle an interface that is a piecewise linear function as long as each linear piece is parallel to one of the coordinate axes, and the pieces in the y-direction occur along the grid-lines of the partition. In other words, all linear pieces in the y-direction will not be allowed to pass through elements. Choosing the y-direction for this restriction is arbitrary, however, and one could also restrict interface pieces in the x-direction to be along the grid-lines, and consequently allow the interface in the y-direction to be immersed.

Then the boundary value problem (1.1)–(1.4) becomes

$$-\nabla \cdot \big(p(\mathbf{x})\nabla u(\mathbf{x})\big) = f(\mathbf{x}), \quad \mathbf{x} = (x, y)^{\mathrm{T}} \in \Omega, \tag{2.24}$$
$$u(x, 0) = g_0(x), \quad u(x, 1) = g_1(x), \quad u(0, y) = h_0(y), \quad u(1, y) = h_1(y), \tag{2.25}$$
$$[u]_\Gamma = 0, \tag{2.26}$$
$$[\mathbf{n} \cdot p\nabla u]_\Gamma = 0, \tag{2.27}$$

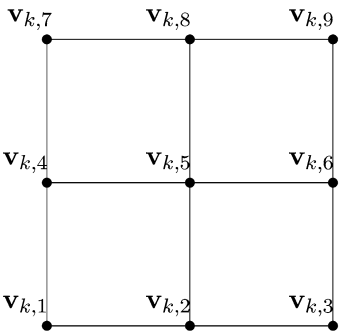

$$\begin{aligned}
\mathbf{v}_{k,1} &= (s_{k,1}, t_{k,1}) \\
\mathbf{v}_{k,2} &= (s_{k,2}, t_{k,1}) \\
\mathbf{v}_{k,3} &= (s_{k,3}, t_{k,1}) \\
\mathbf{v}_{k,4} &= (s_{k,1}, t_{k,2}) \\
\mathbf{v}_{k,5} &= (s_{k,2}, t_{k,2}) \\
\mathbf{v}_{k,6} &= (s_{k,3}, t_{k,2}) \\
\mathbf{v}_{k,7} &= (s_{k,1}, t_{k,3}) \\
\mathbf{v}_{k,8} &= (s_{k,2}, t_{k,3}) \\
\mathbf{v}_{k,9} &= (s_{k,3}, t_{k,3})
\end{aligned}$$

Figure 3. An element $e_k \in \mathcal{T}_h$ with its nine local nodes.

where $\mathbf{n} = (n_1, n_2)^{\mathrm{T}}$ is the unit normal at $\mathbf{x} \in \Gamma$ pointing from Ω_1 to Ω_2. The coefficient p will then be defined by

$$p(x, y) = \begin{cases} p_1 & \text{if } y < \gamma, \\ p_2 & \text{if } y \geqslant \gamma. \end{cases} \tag{2.28}$$

Without loss of generality, we consider forming quadratic IFE spaces on a uniform partition consisting of axially aligned rectangular elements. First, we introduce quadratic node points of the partition in the x- and y-directions by letting

$$\begin{aligned}
x_i &= x_0 + i(h/2), \quad i = 0, 1, \ldots, 2N, \\
y_j &= y_0 + j(h/2), \quad j = 0, 1, \ldots, 2N
\end{aligned}$$

with $h = 1/N$ for an integer N. Then for each pair of integers (i, j), $i, j = 1, 2, \ldots, N$, we let $k = i + (j-1)N$, and let

$$e_k = [x_{2(i-1)}, x_{2i}] \times [y_{2(j-1)}, y_{2j}], \quad i, j = 1, 2, \ldots, N.$$

Finally, we let $\mathcal{T}_h = \bigcup_{k=1}^{N^2} e_k$ to form a partition of $\overline{\Omega}$. We note that the kth element e_k of $\mathcal{T}_h$ is located at the ith column and jth row of the partition.

Each biquadratic element has nine local nodes, and the following notations for the local nodal points on the element e_k is adopted:

$$\begin{aligned}
s_{k,1} &= x_{2(i-1)}, & t_{k,1} &= y_{2(j-1)}, \\
s_{k,2} &= x_{2i-1}, & t_{k,2} &= y_{2j-1}, \\
s_{k,3} &= x_{2i}, & t_{k,3} &= y_{2j},
\end{aligned} \tag{2.29}$$

where $k = i + (j-1)N$. The nine local nodes on the element e_k, $\mathbf{v}_{k,l}$ for $l = 1, \ldots, 9$ can be seen in figure 3 where the node $\mathbf{v}_{k,l}$ is defined by $\mathbf{v}_{k,l} = (s_{k,m}, t_{k,n})$.

As before, to form an IFE spaces, specialized local nodal basis functions will only be used on interface elements which are defined as follows:

Definition 2.2. Let the interface Γ occur along the horizontal line $y = \gamma$. The element $e_k = [x_{2(i-1)}, x_{2i}] \times [y_{2(j-1)}, y_{2j}]$ (where $k = i + (j-1)N$) of the partition $\mathcal{T}_h$ is called an

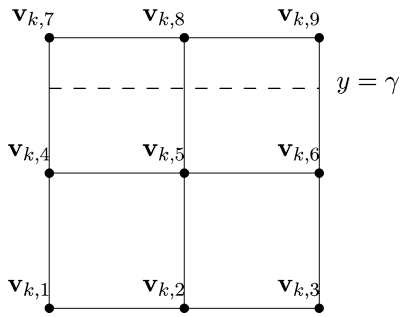

Figure 4. An interface element e_k when the interface Γ is a horizontal line at $y = \gamma$.

interface element if $y_{2(j-1)} < \gamma < y_{2j}$. Any element which is not an interface element will be called a *noninterface element*.

A typical interface element e_k with a horizontal interface at $y = \gamma$ is shown in figure 4.

Then, on a typical noninterface element, the nine biquadratic local nodal basis functions will simply be the standard quadratic FE local basis function defined by

$$\psi_{k,l}(\mathbf{v}_{k,j}) = \begin{cases} 1 & \text{if } j = l, \\ 0 & \text{if } j \neq l, \end{cases} \tag{2.30}$$

for $l = m+3(n-1)$ with $1 \leqslant m, n \leqslant 3$ and $k = i+(j-1)N$. These local basis functions $\psi_{k,l}(x, y)$ can be defined in terms of the standard quadratic FE local basis functions in one dimension as follows

$$\psi_{k,l}(x, y) = \phi_{i,m}(x)\phi_{j,n}(y), \tag{2.31}$$

where $x_{2(i-1)} < x < x_{2i}$ and $y_{2(j-1)} < y < y_{2j}$.

The three types of biquadratic IFE spaces to be introduced below will all be in separable function form, i.e., each local basis function in these spaces will be a product of a function in x variable and a function in y variable. More details will be given about each type of local nodal IFE basis functions in the following subsections.

Additionally, each of these local nodal IFE basis functions will satisfy properties similar to those satisfied by their counterparts of the one-dimensional IFE spaces, such as a partition of unity and consistency with the standard FE local nodal basis functions. Since each of the local nodal IFE basis functions will be a separable function, it is useful to introduce some lemmas regarding these types of functions here.

By direct verifications, we can obtain the following lemma that describes how a group of separable functions can satisfy a partition of unity.

Lemma 2.2. Let $h_{i,j}(x, y)$ for $1 \leqslant i \leqslant m,\ 1 \leqslant j \leqslant n$, be a set of separable functions defined by

$$h_{i,j}(x, y) = f_i(x)g_j(y).$$

If $f_i(x),\ i = 1, \ldots, m$, and $g_j(y),\ j = 1, \ldots, n$, are functions that satisfy

$$\sum_{i=1}^{m} f_i(x) \equiv 1 \quad \text{for all } x \in I_x = [x_1, x_2]$$

and

$$\sum_{j=1}^{m} g_j(y) \equiv 1 \quad \text{for all } y \in I_y = [y_1, y_2],$$

then

$$\sum_{i=1}^{m}\sum_{j=1}^{n} h_{i,j}(x, y) \equiv 1, \quad \text{for all } (x, y) \in \Omega_e = I_x \times I_y. \tag{2.32}$$

It is easy to obtain the following lemma that describes how a separable function can satisfy the two-dimensional interface conditions (2.26) and (2.27).

Lemma 2.3. Let there be an interface Γ that occurs along the the line $y = \gamma$ such that

$$p(x, y) = \begin{cases} p_1, & \text{if } y < \gamma, \\ p_2, & \text{if } y \geqslant \gamma. \end{cases}$$

Also, let $h(x, y) = f(x)g(y)$ where $g(y)$ is piecewise C^1 function defined by

$$g(y) = \begin{cases} g_1(y), & \text{if } y < \gamma, \\ g_2(y), & \text{if } y \geqslant \gamma. \end{cases}$$

If $g(y)$ satisfies the conditions

$$[g]_{y=\gamma} = 0, \qquad \left[pg'(y)\right]_{y=\gamma} = 0,$$

then the function $h(x, y)$ will satisfy (2.26)–(2.27).

Now we are ready to give details about the three two-dimensional biquadratic IFE spaces developed from one dimensional local nodal IFE basis functions $\widetilde{\phi}_{k,i}(x)$, $\overline{\phi}_{k,i}(x)$ and $\widehat{\phi}_{k,i}(x)$.

2.2.1. A two-dimensional hierarchical quadratic IFE space

The first type of biquadratic IFE space is formed by the one-dimensional hierarchical quadratic local nodal basis functions $\widetilde{\phi}_{j,n}(y)$ defined on the interval $[y_{2(j-1)}, y_j]$. If the interface Γ occurs along the line $y = \gamma$ and e_k is an interface element, we defined the biquadratic local nodal IFE basis function $\widetilde{\psi}_{k,l}(x, y)$ by

$$\widetilde{\psi}_{k,l}(x, y) = \phi_{i,m}(x)\widetilde{\phi}_{j,n}(y), \tag{2.33}$$

where $k = i + (j-1)N,\ 1 \leqslant i, j \leqslant N$ and $l = m + 3(n-1),\ 1 \leqslant m, n \leqslant 3$.

These two-dimensional biquadratic local nodal IFE basis functions $\widetilde{\psi}_{k,i}(x, y)$ have properties similar to those of their one-dimensional counterparts. The following theorem establishes that $\widetilde{\psi}_{k,l}(x, y)$ satisfies a partition of unity and that it satisfies the interface conditions (2.26)–(2.27). Additionally, this theorem also points out how these local nodal IFE basis functions are related to the standard FE basis functions. There is a definite similarity between this theorem and theorem 2.2. This is largely due to the fact that the basis function $\widetilde{\psi}_{k,l}(x, y)$ is a separable function and one of its component functions is an one-dimensional quadratic local nodal IFE basis function $\widetilde{\phi}_{j,n}(y)$, both of which are crucial to the proof of this theorem.

Theorem 2.7. Let $e_k = [x_{2(i-1)}, x_{2i}] \times [y_{2(j-1)}, y_{2j}] \in \mathcal{T}_h$ (where $k = i + (j-1)N$) be an interface element. The biquadratic IFE local basis functions $\widetilde{\psi}_{k,l}(x, y),\ l = 1, \ldots, 9$, have the following properties:

1. $\widetilde{\psi}_{k,l}(x, y),\ l = 1, \ldots, 9$, satisfy the interface conditions (2.26)–(2.27).
2. $\sum_{i=l}^{9} \widetilde{\psi}_{k,l}(x, y) \equiv 1$ for all $(x, y) \in e_k$.
3. They are consistent with the standard biquadratic FE functions $\psi_{k,l}(x, y),\ l = 1, \ldots, 9$ in the following ways:

$$\lim_{\gamma \to y_{2(j-1)}} \left(\widetilde{\psi}_{k,l}(x, y)\right) = \psi_{k,l}(x, y),$$
$$\lim_{\gamma \to y_{2j}} \left(\widetilde{\psi}_{k,l}(x, y)\right) = \psi_{k,l}(x, y),$$
$$\lim_{p_2 \to p_1} \left(\widetilde{\psi}_{k,l}(x, y)\right) = \psi_{k,l}(x, y).$$

Proof. Properties 1 and 2 above following directly from lemmas 2.2 and 2.3. Property 3 can be directly verified by using the corresponding results from theorem 2.2. □

Following the same procedure used to construct the one-dimensional IFE space $\widetilde{S}_h(\Omega)$, we can first defined the local IFE space $\widetilde{S}_h^2(e_k)$ for each element $e_k \in \mathcal{T}_h$ as follows:

$$\widetilde{S}_h^2(e_k) = \begin{cases} \text{span}\{\psi_{k,l}(x, y),\ l = 1, 2, \ldots, 9\}, & \text{if } e_k \text{ is a noninterface element,} \\ \text{span}\{\widetilde{\psi}_{k,l}(x, y),\ l = 1, 2, \ldots, 9\}, & \text{if } e_k \text{ is an interface element.} \end{cases}$$

Then we can use $\widetilde{S}_h^2(e_k)$ to form a global nodal basis function for each node in the partition. Finally, we can define the hierarchical two-dimensional biquadratic IFE space $\widetilde{S}_h^2(\Omega)$ as the linear space spanned by these global nodal basis functions.

2.2.2. A biquadratic IFE space with extra continuity

The next type of biquadratic IFE space is to be constructed from the one dimensional quadratic local nodal IFE basis function with extra continuity properties, $\overline{\phi}_{j,n}(y)$

defined on the interval $[y_{2(j-1)}, y_j]$. Specifically, for a typical interface element $e_k \in \mathcal{T}_h$, we define nine quadratic nodal basis functions as follows:

$$\overline{\psi}_{k,l}(x, y) = \phi_{i,m}(x)\overline{\phi}_{j,n}(y) \tag{2.34}$$

where $k = i + (j-1)N,\ 1 \leqslant i, j \leqslant N$ and $l = m + 3(n-1),\ 1 \leqslant m, n \leqslant 3$.

Like $\widetilde{\psi}_{k,l}(x, y)$, the biquadratic local nodal IFE basis functions $\overline{\psi}_{k,l}(x, y)$ also have properties similar to those of their one-dimensional counterparts $\overline{\phi}_{j,n}(y)$ as stated in the following theorem.

Theorem 2.8. Let $e_k = [x_{2(i-1)}, x_{2i}] \times [y_{2(j-1)}, y_{2j}] \in \mathcal{T}_h$ (where $k = i + (j-1)N$) be an interface element. The biquadratic IFE local basis functions $\overline{\psi}_{k,l},\ l = 1, \ldots, 9$, have the same properties as those of $\widetilde{\psi}_{k,l},\ l = 1, \ldots, 9$, stated in theorem 2.7.

Now, we can define a local IFE space $\overline{S}_h^2(e_k)$ for each element $e_k \in \mathcal{T}_h$ as follows:

$$\overline{S}_h^2(e_k) = \begin{cases} span\{\psi_{k,l}(x, y), l = 1, 2, \ldots, 9\}, & \text{if } e_k \text{ is a noninterface element,} \\ span\{\overline{\psi}_{k,l}(x, y), l = 1, 2, \ldots, 9\}, & \text{if } e_k \text{ is an interface element.} \end{cases}$$

Then we can use $\overline{S}_h^2(e_k)$ to form a global nodal basis function for each node in the partition. Finally, we can define the two-dimensional biquadratic IFE space $\overline{S}_h^2(\Omega)$ with extra continuity as the linear space spanned by these global nodal basis functions.

2.2.3. A biquadratic IFE finite element space using local refinement

The last type of biquadratic finite element space considered here is derived by using the one dimensional quadratic local nodal IFE basis function $\widehat{\phi}_{j,n}(y)$. Recall that, in constructing the basis function $\widehat{\phi}_{j,n}(y)$, the element $e_j = [y_{2(j-1)}, y_{2j}]$ is first subdivided into two subelements, $[y_{2(j-1)}, \gamma]$ and $[\gamma, y_{2j}]$, where $y = \gamma$ is the interface. Then four basis functions are introduced onto the element e_j where each basis function satisfied four local nodal value specifications (two on each subelement) and two interface conditions. In two dimensions, when there is an interface at $y = \gamma$, the interface element $e_k = [x_{2(i-1)}, x_{2i}] \times [y_{2(j-1)}, y_{2j}]$ (where $k = i + (j-1)N$) will have 12 local nodes. Here, the nodal points in the x- and y-directions of a typical interface element are

$$\begin{aligned} s_{k,1} &= x_{2(i-1)}, & \hat{t}_{k,1} &= y_{2(j-1)}, \\ s_{k,2} &= x_{2i-1}, & \hat{t}_{k,2} &= (y_{2(j-1)} + \gamma)/2, \\ s_{k,3} &= x_{2i}, & \hat{t}_{k,3} &= (\gamma + y_{2j})/2, \\ & & \hat{t}_{k,4} &= y_{2j}. \end{aligned} \tag{2.35}$$

See the illustration in figure 5.

Notice that there are four nodal points in the y-direction since four nodal value specifications are needed in the direction that crosses the interface so that the inter-

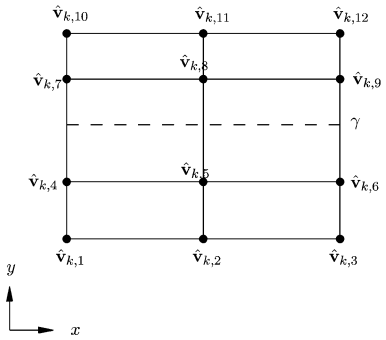

$$
\begin{aligned}
\hat{\mathbf{v}}_{k,1} &= (s_{k,1}, \hat{t}_{k,1}), \quad & \hat{\mathbf{v}}_{k,7} &= (s_{k,1}, \hat{t}_{k,3}),\\
\hat{\mathbf{v}}_{k,2} &= (s_{k,2}, \hat{t}_{k,1}), \quad & \hat{\mathbf{v}}_{k,8} &= (s_{k,2}, \hat{t}_{k,3}),\\
\hat{\mathbf{v}}_{k,3} &= (s_{k,3}, \hat{t}_{k,1}), \quad & \hat{\mathbf{v}}_{k,9} &= (s_{k,3}, \hat{t}_{k,3}),\\
\hat{\mathbf{v}}_{k,4} &= (s_{k,1}, \hat{t}_{k,2}), \quad & \hat{\mathbf{v}}_{k,10} &= (s_{k,1}, \hat{t}_{k,4}),\\
\hat{\mathbf{v}}_{k,5} &= (s_{k,2}, \hat{t}_{k,2}), \quad & \hat{\mathbf{v}}_{k,11} &= (s_{k,2}, \hat{t}_{k,4}),\\
\hat{\mathbf{v}}_{k,6} &= (s_{k,3}, \hat{t}_{k,2}), \quad & \hat{\mathbf{v}}_{k,12} &= (s_{k,3}, \hat{t}_{k,4}).
\end{aligned}
$$

Figure 5. The local quadratic nodes $\hat{\mathbf{v}}_{k,l}$ for $\widehat{\psi}_{k,l}(x, y)$ on the interface element e_k with interface $y = \gamma$.

face conditions may be satisfied. Then we define 12 local nodal IFE basis functions $\widehat{\psi}_{k,l}(x, y),\ l = 1, \ldots, 12$, in an interface element e_k as

$$\widehat{\psi}_{k,l}(x, y) = \phi_{i,m}(x)\widehat{\phi}_{j,n}(y) \tag{2.36}$$

where $k = i + (j-1)N,\ 1 \leqslant i, j \leqslant N$ and $l = m + 4(n-1),\ 1 \leqslant m \leqslant 3,\ 1 \leqslant n \leqslant 4$.

While the construction of the local nodal IFE basis functions $\widehat{\psi}_{k,l}(x, y)$ is similar to the construction used for both $\widetilde{\psi}_{k,l}(x, y)$ and $\overline{\psi}_{k,i}(x, y)$, these local basis functions do not satisfy all of the same properties as $\widetilde{\psi}_{k,l}(x, y)$ and $\overline{\psi}_{k,i}(x, y)$. For example, these local basis functions do not have a direct relationship with the standard quadratic finite element local basis functions. However, since the construction does result in a separable function, then lemmas 2.2 and 2.3 can again be used to prove the following theorem.

Theorem 2.9. Let $e_k = [x_{2(i-1)}, x_{2i}] \times [y_{2(j-1)}, y_{2j}] \in \mathcal{T}_h$ (where $k = i + (j-1)N$) be an interface element. The biquadratic IFE local basis functions $\widehat{\psi}_{k,l},\ l = 1, \ldots, 12$, have the following properties:

1. They satisfy the interface conditions (2.26)–(2.27).
2. $\sum_{i=l}^{12} \widehat{\psi}_{k,l}(x, y) \equiv 1$ for all $(x, y) \in e_k$.

Now, we are ready to define the IFE space based on local refinement. We first defined a local IFE space $\widehat{S}_h^2(e_k)$ for each element $e_k \in \mathcal{T}_h$ as follows:

$$\widehat{S}_h^2(e_k) = \begin{cases} span\{\psi_{k,l}(x, y), l = 1, 2, \ldots, 9\}, & \text{if } e_k \text{ is a noninterface element,}\\ span\{\widehat{\psi}_{k,l}(x, y), l = 1, 2, \ldots, 12\}, & \text{if } e_k \text{ is an interface element.} \end{cases}$$

Then we can use $\widehat{S}_h^2(e_k)$ to form a global nodal basis function for each node in the partition. Finally, we can define the two-dimensional biquadratic IFE space $\widehat{S}_h^2(\Omega)$ based upon local refinement as the linear space spanned by these global nodal basis functions.

3. Numerical experiments of the quadratic and biquadratic IFE spaces

In this section, we investigate numerically the approximation capability of the IFE spaces introduced in the previous section. We consider errors in both the interpolants and finite element solutions generated in these IFE spaces. These numerical experiments can provide a guideline for the related error estimation of these IFE spaces that will be presented in a forthcoming paper.

We use $I_h u(x)$ to denote the interpolant of a function $u(x)$ in an IFE space with a mesh size h, and use $u_h(x)$ to denote the finite element solution of an interface value problem in an IFE space with a mesh size h where the interface value problem has an exact solution $u(x)$. Similar notation will be used in the two-dimensional case. To measure the errors, we use the following norms in the involved Sobolev spaces:

$$\begin{aligned} &\|u\|_\infty = \operatorname*{ess\,sup}_{\mathbf{x}\in\Omega} \big|u(\mathbf{x})\big|, \qquad \|u\|_0 = \left(\int_\Omega u^2\, d\mathbf{x}\right)^{1/2}, \\ &\|u\|_1 = \left(\|u\|_0^2 + \left\|u'\right\|_0^2\right)^{1/2}. \end{aligned} \tag{3.1}$$

Using these norms, we can measure the magnitudes of the errors in the interpolants and finite element solutions with the following quantities:

$$E_{h,s}(I_h u) = \|u - I_h u\|_s \quad \text{or} \quad E_{h,s}(u_h) = \|u - u_h\|_s \tag{3.2}$$

with $s = 0, 1$, or $s = \infty$. When it is clear which norm is used, the error will simply be referred to as $E_h(I_h u)$ or $E_h(u_h)$. Similarly, if it is clear from the context whether we consider the error in an interpolant or the error in a finite element solution, then the error will be referred to as E_h or $E_{h,s}$. We say that an approximation (either $I_h u$ or u_h) is of order r if

$$E_h \approx C h^r \tag{3.3}$$

for some constant C.

In our numerical experiments, we identify the order approximately by carrying out a least squares regression on a set of values of $\log E_h$ generated for various values of h. To assess the errors numerically, we approximate L^∞ error, $E_{h,\infty}$, by evaluating $|u - u_h|$ (or $|u - I_h u|$) t (an integer sufficiently large) times on each element and then using the maximum of these values as of $|u - u_h|$. However, an interface element is treated through two natural subelements: the one contained in Ω_1 and the other contained in Ω_2.

3.1. Numerical results in one dimension

Recall that we use $\overline{S}_h(\Omega)$, $\widehat{S}_h(\Omega)$ and $\widetilde{S}_h(\Omega)$ to denote that IFE spaces spanned by the nodal basis functions $\overline{\phi}_i(x)$, $\widehat{\phi}_i(x)$ and $\widetilde{\phi}_i(x)$, respectively. Numerical results from these IFE spaces are to be considered. First, we introduce two test functions emphasizing different features in order to provide a good testing ground for these IFE spaces. Then the errors in the interpolants of these test functions in the IFE spaces are presented. Finally, we look at the errors in the Galerkin finite element solutions in these IFE spaces

for the interface problems defined in the ways such that these test functions are their exact solutions.

Even though all the functions in the three IFE spaces share some fundamental properties such as being able to satisfy the jump conditions, functions in these IFE spaces are indeed different in the continuity of their flux across the interface. It is therefore interesting to see how the IFE spaces can perform in generating approximations to test functions whose fluxes have different continuities.

Two test functions are considered. For the first one, $u_1(x)$, we let it be the exact solution of the interface problem (2.1)–(2.4) with homogeneous Dirichlet boundary conditions when the right hand side function is defined by

$$f_1(x) = \mathrm{e}^x \tag{3.4}$$

and the interface is located at $\alpha = 1/\pi$. We can easily check that function $u_1(x)$ can be given explicitly with the following formula:

$$u_1(x) = \begin{cases} \dfrac{1}{-D}\big(\mathrm{e}^x(\alpha p_2 + p_1) + \alpha(p_1 - p_2) - p_1 \\ \quad + x\big(\mathrm{e}^\alpha(p_1 - p_2) + p_2 - \mathrm{e}p_1\big)\big), \quad \text{if } x < \alpha, \\ \dfrac{p_1}{p_2 D}\big(\mathrm{e}^x p_1 - \alpha\big(\mathrm{e}^x - \mathrm{e}\big)(p_1 - p_2) \\ \quad + \mathrm{e}^\alpha(p_1 - p_2)(x - 1) + p_2(x - 1) - \mathrm{e}p_1 x\big), \quad \text{if } x \geqslant \alpha, \end{cases} \tag{3.5}$$

where $D = p_1 + \alpha(p_2 - p_1)$.

The second function, $u_2(x)$, is defined as the exact solution of the interface problem (2.1)–(2.4) with homogeneous Dirichlet boundary conditions when the right-hand side function is defined by

$$f_2(x) = \begin{cases} \mathrm{e}^x, & x < 1/\pi, \\ -\mathrm{e}^{1-x}, & x \geqslant 1/\pi, \end{cases} \tag{3.6}$$

and the interface is located at $\alpha = 1/\pi$. The formula for the function $u_2(x)$ can also be derived by using Green's functions.

Since $u_1(x)$ and $u_2(x)$ are both solutions of the interface problem (2.1)–(2.4) with corresponding right-hand side functions, then it follows that $u_1(x)$ and $u_2(x)$ both satisfy the interface jump conditions (2.3)–(2.4). However, since $f_1(x)$ is continuous at the interface $\alpha = 1/\pi$ while $f_2(x)$ is not, it follows that $pu_1''(x)$ is continuous at the interface and $pu_2''(x)$ is not.

3.1.1. Interpolation accuracy of the one-dimensional IFE spaces

In this group of numerical experiments, we generate interpolants of the test functions $u_1(x)$ and $u_2(x)$ in the IFE spaces $\widetilde{S}_h(\Omega)$, $\overline{S}_h(\Omega)$ and $\widehat{S}_h(\Omega)$ respectively with a sequence of partition sizes $h = 1/8,\ 1/16,\ 1/32,\ 1/64,\ 1/128$ and $h = 1/256$. The errors in the interpolants $I_h u_1$ and $I_h u_2$ for the case in which the coefficient p has a ratio of $p_2/p_1 = 10$ are presented in tables 8–10 of the appendix at the end of this article. We

Table 1
The orders of the IFE interpolants $I_h u_i,\ i = 1, 2$, generated in the IFE spaces $\widetilde{S}_h(\Omega)$, $\overline{S}_h(\Omega)$ and $\widehat{S}_h(\Omega)$ with $p_2/p_1 = 10$.

		u_1		u_2	
IFE space	Error	C	r	C	r
$\widetilde{S}_h(\Omega)$	$E_{h,\infty}$	0.016	1.983	0.024	1.954
	$E_{h,0}$	0.006	2.436	0.009	2.408
	$E_{h,1}$	0.093	1.577	0.141	1.554
$\overline{S}_h(\Omega)$	$E_{h,\infty}$	0.010	2.973	0.008	1.764
	$E_{h,0}$	0.004	2.990	0.003	2.235
	$E_{h,1}$	0.025	1.991	0.045	1.368
	$E_{h,\infty}$	0.010	2.973	0.010	2.972
$\widehat{S}_h(\Omega)$	$E_{h,0}$	0.003	2.971	0.003	2.969
	$E_{h,1}$	0.022	1.973	0.022	1.972

then apply linear regression on these data to estimate the orders of $I_h u_1$ and $I_h u_2$, the related results are listed in table 1, where the parameters C and r are defined in (3.3).

From table 8, we can see the errors in $I_h u_i \in \widetilde{S}_h(\Omega),\ i = 1, 2$, do not always decrease as h decreases. However, the errors do tend to decrease in an oscillatory fashion which becomes more apparent when we look at the numerical results generated with a larger set of values of h. From table 1, we also see that the orders of $I_h u_i \in \widetilde{S}_h(\Omega),\ i = 1, 2$, are worse than would be expected for a FE space generated by quadratic polynomials. While the orders of $E_{h,0}$ and $E_{h,1}$ only appear to be a little more than one fourth of an order less than what one would expect, the orders of $E_{h,\infty}$ appear to be a little more than three-fourths of an order less than what is expected.

The errors of the interpolants $I_h u_i \in \overline{S}_h(\Omega),\ i = 1, 2$, are shown in table 9. According to table 9, the errors in the interpolant $I_h u_1$ appear to decrease whenever h decreases while the errors in the interpolant $I_h u_2$ decrease only in an oscillatory fashion. Also, the errors in $I_h u_1$ appear to be much smaller than those for the interpolant $I_h u_2$, and the magnitude of the errors in $I_h u_2$ are similar to those obtained when using the hierarchical IFE space $\widetilde{S}_h(\Omega)$. From table 1, we see that the orders for the interpolant $I_h u_1$ agrees with our expectation for a FE space using quadratic polynomials, while the orders of $I_h u_2$ indicate that the IFE space $\widetilde{S}_h(\Omega)$ has a weaker approximation capability than the usual quadratic FE space.

From table 10, we notice that the errors in $I_h u_i \in \widehat{S}_h(\Omega),\ i = 1, 2$, decrease monotonically as the partition size h becomes smaller, and the orders of $I_h u_i \in \widehat{S}_h(\Omega),\ i = 1, 2$, are in agreement with those generated in the usual quadratic FE space.

The satisfactory performance of interpolants from the IFE basis space $\widehat{S}_h(\Omega)$ is not surprising because the IFE space is very close to a standard FE space based on a usual body fit partition in which each element has to be on one side of the interface in

Table 2
Approximation capability of interpolants in the three one-dimensional IFE spaces.

	$\widetilde{S}_h(\Omega)$	$\overline{S}_h(\Omega)$	$\widehat{S}_h(\Omega)$
u_1	weaker than expected	as expected	as expected
u_2	weaker than expected	weaker than expected	as expected

a certain sense. Recall that the basis functions $\widehat{\phi}_i(x)$ that span the IFE space $\widehat{S}_h(\Omega)$ are fundamentally different from the basis functions that span either $\widetilde{S}_h(\Omega)$ or $\overline{S}_h(\Omega)$ because of the way that the nodal values are handled on the interface element. Because of the nodal value specifications used for the local basis functions $\widehat{\phi}_{k,i}(x)$, their construction is equivalent to forming quadratic functions on each half of the element such that they are linear combinations of the standard FE quadratic basis functions on these two subelements. In the formation of these linear combinations of quadratic functions, it becomes apparent that instead of six basis functions being specified, only four are needed due to the interface jump conditions given. Finally, because the interface occurs at the "node" between the two subelements, this IFE space is essentially close to a FE space based on a body fit partition where the interface is located at one of the nodes.

Similar behaviors are observed in the errors of the interpolants of $u_1(x)$ and $u_2(x)$ generated in the IFE spaces $\widetilde{S}_h(\Omega)$, $\overline{S}_h(\Omega)$ and $\widehat{S}_h(\Omega)$ for the case in which the coefficient p has a larger ratio $p_2/p_1 = 10000$. The related datum are omitted to reduce the presentation space.

In table 2, we summarize our observations about the approximation capabilities of the iterpolants in the various IFE spaces.

3.1.2. Accuracy of IFE methods for one-dimensional interface problems

Now we look at errors in the approximate solution of the interface problem (2.1)–(2.4) generated by the Galerkin method with the three one-dimensional IFE spaces introduced in section 2. We will use the same test functions as in the previous section so that $u_1(x)$ is the exact solution to (2.1)–(2.4) when the function on the right-hand side is defined by (3.4) and $u_2(x)$ is the exact solution to (2.1)–(2.4) when the right-hand side function is defined by (3.6).

The errors in the finite element solution u_{1h} and u_{2h} generated in the IFE spaces $\widetilde{S}_h(\Omega)$, $\overline{S}_h(\Omega)$ and $\widehat{S}_h(\Omega)$ for the case in which the coefficient p has a ratio $p_2/p_1 = 10$ are list 11–13. Applying linear regression generates the estimates of the orders of these IFE solutions listed in table 3.

The behaviors of the errors in the IFE solutions $u_{1h}(x)$ and $u_{2h}(x)$ are similar to their interpolation counterparts generated in the corresponding IFE spaces. The estimates on the orders of these IFE solutions also have values similar to those of the IFE interpolants reported in the previous section.

To achieve the optimal order of accuracy in the IFE solution generated from $\overline{S}_h(\Omega)$, the interface problem needs to have one extra continuity across the interface. However,

Table 3
The orders of IFE solutions $u_{ih}, i = 1, 2$, generated in the IFE spaces $\widetilde{S}_h(\Omega)$, $\overline{S}_h(\Omega)$ and $\widehat{S}_h(\Omega)$ with $p_2/p_1 = 10$.

		u_1		u_2	
IFE space	Error	C	r	C	r
$\widetilde{S}_h(\Omega)$	$E_{h,\infty}$	0.010	2.042	0.016	2.022
	$E_{h,0}$	0.008	2.594	0.012	2.570
	$E_{h,1}$	0.073	1.663	0.111	1.641
$\overline{S}_h(\Omega)$	$E_{h,\infty}$	0.010	2.971	0.007	1.842
	$E_{h,0}$	0.004	2.981	0.003	2.291
	$E_{h,1}$	0.024	1.983	0.046	1.408
$\widehat{S}_h(\Omega)$	$E_{h,\infty}$	0.010	2.971	0.010	2.971
	$E_{h,0}$	0.003	2.971	0.003	2.969
	$E_{h,1}$	0.022	1.973	0.022	1.972

Table 4
The order of the IFE solutions $u_{ih}, i = 1, 2$, generated in IFE space $\widetilde{S}_h(\Omega)$ with $p_2/p_1 = 10000$.

		u_1		u_2	
IFE space	Error	C	r	C	r
$\widetilde{S}_h(\Omega)$	$E_{h,\infty}$	0.010	2.971	0.010	2.971
	$E_{h,0}$	0.003	2.961	0.003	2.969
	$E_{h,1}$	0.022	1.971	0.022	1.971

this is not an essential limitation of this IFE space because we can always transform the interface problem to an equivalent problem that has the required continuity in the flux by applying the pertinent homogenization.

For the case in which the coefficient p has a larger ratio $p_2/p_1 = 10000$, the errors in the IFE solutions $u_{1h}(x)$ and $u_{2h}(x)$ generated in the IFE spaces $\overline{S}_h(\Omega)$ and $\widehat{S}_h(\Omega)$ behave in a way similar to what observed for the case in which p has a smaller ratio $p_2/p_1 = 10$. However, see table 14, we note that the errors of the IFE solution $u_{ih}(x)$ generated in the IFE space $\widetilde{S}_h(\Omega)$ appear to decrease steadily as h decreases. The estimates of the orders of these IFE solutions are listed in table 4 from which we can see that the IFE solutions generated from this space have orders comparable to the standard quadratic FE solutions. In this case, the IFE solutions seem to have a better approximation capability than interpolants from this IFE space, and it is interesting to carry out pertinent analysis to understand this phenomenon.

We finally summarize the approximation capability of the IFE solutions of the one-dimensional test interface problems in table 5.

Table 5
Approximation capability of the IFE solutions of the one-dimensional test interface problems.

	$\widetilde{S}_h(\Omega)$	$\overline{S}_h(\Omega)$	$\widehat{S}_h(\Omega)$
u_1	weaker than expected	as expected	as expected
u_2	weaker than expected	weaker than expected	as expected

3.2. Numerical results in two dimensions

As was mentioned in section 2, we will restrict our attention to the case when the interface is a horizontal line and the domain Ω is the unit square (i.e., see the BVP (2.24)–(2.27) for a more thorough description). We start by choosing suitable test functions. Since each IFE space introduced in the previous sections is made up of basis functions which satisfy the interface conditions (2.26)–(2.27), we naturally need to make sure that the test functions will also satisfy these conditions. In two dimensions, when the interface is a horizontal line, this means that a function u will satisfy (2.26)–(2.27) if $u \in C(\Omega)$ and $p\partial u/\partial y \in C(\Omega)$. Then we would like also consider the continuity of $(\partial/\partial y)(p\partial u/\partial y)$ across the interface because of the way the IFE space $\overline{S}_h^2(\Omega)$ is constructed. This extra continuity leads us to consider two test functions $u_3(x, y)$ and $u_4(x, y)$ in order to explore the all the possibilities. In addition, these two functions will also be chosen so that they satisfy the BVP (2.24)–(2.27) with the right-hand functions suitably chosen, and with homogeneous Dirichlet boundary conditions and the interface occurring along the horizontal line $y = \mathrm{e}^{-1}$.

Specifically, the general form for the test function $u_j,\ j = 3, 4$, is

$$u_j(x, y) = \begin{cases} \sin(\pi x)\big(a_5y^5 + a_4y^4 + a_3y^3 + a_2y^2 + a_1y + a_0\big), & y < \mathrm{e}^{-1}, \\ \sin(\pi x)\big(b_5y^5 + b_4y^4 + b_3y^3 + b_2y^2 + b_1y + b_0\big), & y \geqslant \mathrm{e}^{-1}. \end{cases} \tag{3.7}$$

The coefficients $a_i,\ i = 0, \ldots, 5$, and $b_i,\ i = 0, \ldots, 5$, will be chosen so that $(\partial/\partial y)(p\partial u_j/\partial y),\ j = 3, 4$ will be discontinuous and continuous across the interface, respectively.

3.2.1. Interpolation accuracy of the two-dimensional IFE spaces

In this section we will investigate the approximation capability of the interpolants from the IFE spaces for the two test functions. The errors in the interpolants I_hu_3 and I_hu_4 are listed in tables 15–17. Applying linear regression to these data, we obtain estimates of orders of these interpolants listed in table 6.

From these numerical estimates of the orders in the interpolants, we can see that from the point of view of approximating the test functions u_3 and u_4 as L^2 functions by their interpolants, the IFE space $\widetilde{S}_h^2(\Omega)$ behaves like the usual quadratic FE space. However, when trying to approximate u_3 and u_4 either as L^∞ or H^2 functions, this IFE space does not seem to be able to generate interpolants with accuracies up to those from the usual quadratic FE space.

Table 6
The orders of the IFE interpolants $I_h u_i(x, y),\ i = 3, 4$, generated in IFE spaces $\widetilde{S}_h(\Omega)$, $\overline{S}_h(\Omega)$ and $\widehat{S}_h(\Omega)$ with $p_2/p_1 = 10$.

		u_3		u_4	
IFE space	Error	C	r	C	r
$\widetilde{S}_h(\Omega)$	$E_{h,\infty}$	8.789	2.633	4.720	2.234
	$E_{h,0}$	7.405	2.980	9.595	2.934
	$E_{h,1}$	35.985	1.876	25.053	1.606
$\overline{S}_h(\Omega)$	$E_{h,\infty}$	3.112	2.172	37.933	3.001
	$E_{h,0}$	6.247	2.898	11.131	2.988
	$E_{h,1}$	16.171	1.563	73.998	1.993
$\widehat{S}_h(\Omega)$	$E_{h,\infty}$	25.555	3.000	37.933	3.001
	$E_{h,0}$	7.458	2.985	10.980	2.985
	$E_{h,1}$	50.038	1.992	73.668	1.992

We note that these orders indicate that the interpolant $I_h u_3 \in \overline{S}_h^2(\Omega)$ can not approximate u_3 as well as the interpolant generated from the standard quadratic FE space even rough the error of $I_h u_3$ in the L^2 norm seems to be up to our expectation. On the other hand, for the test function u_4, the IFE space $\overline{S}_h^2(\Omega)$ seems to have an approximation capability comparable to that of the standard quadratic FE space.

The performance of the interpolants generated from the IFE space $\widehat{S}_h^2(\Omega)$ for both test functions is obviously comparable to those from the standard FE space. Overall, from these numerical experiments, we notice that the biquadratic IFE spaces behave very much like their corresponding one dimensional IFE spaces.

3.2.2. Accuracy of IFE methods for two-dimensional interface problems

In this section we turn our attention to the errors that occur when approximating the solutions of the interface problem (2.24)–(2.27) with homogeneous Dirichlet boundary conditions by finite element solutions generated from the two-dimensional IFE spaces $\widetilde{S}_h^2(\Omega)$, $\overline{S}_h^2(\Omega)$ and $\widehat{S}_h^2(\Omega)$. The same test functions used for investigating the interpolation approximation capability in the previous subsection are used again here to explore the performance of each of the IFE spaces when used with the Galerkin method. Here each test function $u_i,\ i = 3, 4$, will be matched with an appropriate function $f_i(x, y)$ so that the corresponding u_i is the exact solution of the interface problem when each f_i occurs as the function on the right hand side of PDE in the interface problem (2.24)–(2.27).

The errors in the IFE solutions u_{3h} and u_{4h} are listed in tables 18–20. Applying linear regression to these data, we obtain estimates of orders of these IFE solutions listed in table 7.

We note that, in the L^2 norm, the performance of the IFE solutions generated from the IFE space $\widetilde{S}_h(\Omega)$ match that generated from a standard quadratic FE space. For test functions u_4, in both L^∞ and H^1 norms, the order of the IFE solutions generated from

Table 7
The orders of the IFE $u_{ih}(x, y)$, $i = 3, 4$, generated in IFE spaces $\widetilde{S}_h(\Omega)$, $\overline{S}_h(\Omega)$ and $\widehat{S}_h(\Omega)$ with $p_2/p_1 = 10$.

		u_3		u_4	
IFE space	Error	C	r	C	r
$\widetilde{S}_h(\Omega)$	$E_{h,\infty}$	15.247	2.828	9.265	2.498
	$E_{h,0}$	7.351	2.979	9.487	2.933
	$E_{h,1}$	43.049	1.939	36.617	1.744
$\overline{S}_h(\Omega)$	$E_{h,\infty}$	3.456	2.230	37.916	3.001
	$E_{h,0}$	6.417	2.913	11.056	2.987
	$E_{h,1}$	16.916	1.585	73.738	1.992
$\widehat{S}_h(\Omega)$	$E_{h,\infty}$	25.551	3.000	37.907	3.001
	$E_{h,0}$	7.448	2.985	10.966	2.985
	$E_{h,1}$	50.038	1.992	73.687	1.992

the IFE space $\widetilde{S}_h(\Omega)$ seem to be lower than than those from a standard quadratic FE space. It is interesting to see that, in the IFE space $\widetilde{S}_h(\Omega)$, the IFE solution to u_3 has a higher order than the IFE interpolant of u_3.

In both L^∞ and H^1 norms, the order of the IFE solutions generated from $\overline{S}_h^2(\Omega)$ for u_3 are lower than that generated from the standard quadratic FE space. Again, as we have commented for the similar phenomenon in one dimension, this minor limitation can be alleviated by transforming the interface problem to an equivalent problem with the extra continuity by a suitable homogenization. On the other hand, in the L^2 norm, the IFE solution of u_3 seems to have the order as expected. The orders of the IFE solutions from $\overline{S}_h^2(\Omega)$ for u_4 match those of the standard quadratic FE space.

As for the IFE solutions generated from the IFE space $\widehat{S}_h^2(\Omega)$, there is nothing remarkable to say here other than that again their performance is comparable to the standard FE solutions based on body fit partitions.

Overall, we conclude that, when used to solve the test interface problems, the approximation capability of the two dimensional quadratic IFE spaces is similar to that of the one-dimensional IFE spaces.

4. Conclusions

In this paper, we have developed three one-dimensional quadratic immersed finite element spaces $\widetilde{S}_h(\Omega)$, $\overline{S}_h(\Omega)$, $\widehat{S}_h(\Omega)$ and their two-dimensional tensor product extensions for solving elliptic interface problems. These IFE spaces have the following features:

- Their partition can be independent of the interface location.
- These IFE spaces are closely related with the standard quadratic FE because they use the standard quadratic local basis functions on most of the elements, and IFE spaces $\widetilde{S}_h(\Omega)$, $\overline{S}_h(\Omega)$ even reduce to the standard quadratic FE space when the discontinuity

in the coefficient disappears or when the discontinuity happens on the edges of the elements in the partition. This feature can make the adoption of these IFE spaces easy because the users only need to modify the local basis subroutines of a standard quadratic FE package.

- Both $\overline{S}_h(\Omega)$ and $\widehat{S}_h(\Omega)$ demonstrate optimal approximation capability expected from a FE space using quadratic polynomials. The IFE space $\widetilde{S}_h(\Omega)$ seems to have a sub-optimal approximation capability. From our numerical experiments, we conjecture that its orders are one half less than the optimal, and we are carrying out related analysis to confirm this.
- We note that to achieve the optimal order of accuracy from the IFE space $\overline{S}_h(\Omega)$, the interface problem needs to have one extra continuity across the interface. However, this is not an essential limitation of this IFE space because we can always transform the interface problem to an equivalent problem that has the required continuity by applying the pertinent homogenization.
- From the point of view of approximation capability, $\overline{S}_h(\Omega)$, $\widehat{S}_h(\Omega)$ are better than the IFE space $\widetilde{S}_h(\Omega)$. However, we think $\widetilde{S}_h(\Omega)$ is still a competitive IFE space. Fist its orders (in both L^2 and H^1 norms) are not too far below the optimal. Second, its hierarchical structure has the potential to be employed in the adaptive procedure according the polynomial degree.

We would like emphasize that which IFE space to use should be determined by the nature of the application.

Acknowledgement

We would like to thank the referees for their comments and suggestions that were of great help in revising this article.

Appendix

This section contains data of the numerical experiments presented in the previous section. In all of these data tables, $x.xxx(y)$ means $x.xxx \times 10^y$.

Table 8
Errors in $I_h u_i$, $i = 1, 2$, generated in the quadratic IFE space $\widetilde{S}_h(\Omega)$ with $p_2/p_1 = 10$.

h	$E_{h,\infty}(I_h u_1)$	$E_{h,0}(I_h u_1)$	$E_{h,1}(I_h u_1)$	$E_{h,\infty}(I_h u_2)$	$E_{h,0}(I_h u_2)$	$E_{h,1}(I_h u_2)$
1/8	2.398(−4)	4.950(−5)	2.667(−3)	3.680(−4)	7.671(−5)	4.159(−3)
1/16	5.293(−5)	4.353(−6)	1.162(−3)	8.547(−5)	6.827(−6)	1.881(−3)
1/32	2.612(−5)	1.628(−6)	6.682(−4)	4.368(−5)	2.714(−6)	1.118(−3)
1/64	9.317(−6)	5.441(−7)	2.770(−4)	1.580(−5)	9.220(−7)	4.695(−4)
1/128	2.177(−7)	9.784(−9)	8.387(−6)	3.702(−7)	1.626(−8)	1.401(−5)
1/256	5.287(−7)	1.763(−8)	2.912(−5)	9.018(−7)	3.008(−8)	4.966(−5)

Table 9
Errors in $I_h u_i,\ i = 1, 2$, generated in the quadratic IFE space $\overline{S}_h(\Omega)$ with $p_2/p_1 = 10$.

h	$E_{h,\infty}(I_h u_1)$	$E_{h,0}(I_h u_1)$	$E_{h,1}(I_h u_1)$	$E_{h,\infty}(I_h u_2)$	$E_{h,0}(I_h u_2)$	$E_{h,1}(I_h u_2)$
1/8	1.903(−5)	7.375(−6)	3.844(−4)	4.360(−4)	9.072(−5)	4.918(−3)
1/16	2.600(−6)	9.562(−7)	9.934(−5)	1.968(−5)	1.790(−6)	4.467(−4)
1/32	3.293(−7)	1.194(−7)	2.482(−5)	1.492(−5)	9.327(−7)	3.829(−4)
1/64	4.144(−8)	1.499(−8)	6.236(−6)	9.794(−6)	5.718(−7)	2.911(−4)
1/128	5.197(−9)	1.872(−9)	1.554(−6)	5.703(−7)	2.499(−8)	2.153(−5)
1/256	6.532(−10)	2.356(−10)	3.909(−7)	7.612(−7)	2.539(−8)	4.192(−5)

Table 10
Errors in $I_h u_i,\ i = 1, 2$, generated in the quadratic IFE space $\widehat{S}_h(\Omega)$ with $p_2/p_1 = 10$.

h	$E_{h,\infty}(I_h u_1)$	$E_{h,0}(I_h u_1)$	$E_{h,1}(I_h u_1)$	$E_{h,\infty}(I_h u_2)$	$E_{h,0}(I_h u_2)$	$E_{h,1}(I_h u_2)$
1/8	1.903(−5)	6.677(−6)	3.499(−4)	1.903(−5)	6.543(−6)	3.431(−4)
1/16	2.600(−6)	9.544(−7)	9.913(−5)	2.600(−6)	9.417(−7)	9.797(−5)
1/32	3.293(−7)	1.192(−7)	2.474(−5)	3.293(−7)	1.176(−7)	2.440(−5)
1/64	4.144(−8)	1.490(−8)	6.182(−6)	4.144(−8)	1.469(−8)	6.094(−6)
1/128	5.197(−9)	1.867(−9)	1.551(−6)	5.197(−9)	1.841(−9)	1.529(−6)
1/256	6.532(−10)	2.347(−10)	3.895(−7)	6.532(−10)	2.314(−10)	3.841(−7)

Table 11
Errors in the IFE solutions $u_{ih},\ i = 1, 2$, generated in the quadratic IFE space $\widetilde{S}_h(\Omega)$ with $p_2/p_1 = 10$.

h	$E_{h,\infty}(u_{1h})$	$E_{h,0}(u_{1h})$	$E_{h,1}(u_{1h})$	$E_{h,\infty}(u_{2h})$	$E_{h,0}(u_{2h})$	$E_{h,1}(u_{2h})$
1/8	1.516(−4)	3.268(−5)	1.521(−3)	2.429(−4)	5.109(−5)	2.389(−3)
1/16	2.553(−5)	4.933(−6)	8.411(−4)	4.116(−5)	7.848(−6)	1.366(−3)
1/32	1.217(−5)	1.604(−6)	3.895(−4)	2.034(−5)	2.676(−6)	6.518(−4)
1/64	3.396(−6)	2.856(−7)	1.090(−4)	5.756(−6)	4.833(−7)	1.845(−4)
1/128	2.173(−7)	9.802(−9)	8.431(−6)	3.689(−7)	1.632(−8)	1.416(−5)
1/256	1.704(−7)	6.591(−9)	9.739(−6)	2.907(−7)	1.124(−8)	1.660(−5)

Table 12
Errors in the IFE solutions $u_{ih},\ i = 1, 2$, generated in the quadratic IFE space $\overline{S}_h(\Omega)$ with $p_2/p_1 = 10$.

h	$E_{h,\infty}(u_{1h})$	$E_{h,0}(u_{1h})$	$E_{h,1}(u_{1h})$	$E_{h,\infty}(u_{2h})$	$E_{h,0}(u_{2h})$	$E_{h,1}(u_{2h})$
1/8	1.893(−5)	7.019(−6)	3.678(−4)	3.048(−4)	7.453(−5)	4.114(−3)
1/16	2.593(−6)	9.557(−7)	9.926(−5)	1.738(−5)	1.621(−6)	4.293(−4)
1/32	3.289(−7)	1.194(−7)	2.481(−5)	1.238(−5)	8.270(−7)	3.628(−4)
1/64	4.141(−8)	1.496(−8)	6.219(−6)	6.330(−6)	4.248(−7)	2.337(−4)
1/128	5.195(−9)	1.870(−9)	1.552(−6)	5.404(−7)	2.766(−8)	2.445(−5)
1/256	6.532(−10)	2.350(−10)	3.901(−7)	3.670(−7)	1.457(−8)	2.711(−5)

Table 13
Errors in the IFE solutions $u_{ih},\ i = 1, 2$, generated in the quadratic IFE space $\widehat{S}_h(\Omega)$ with $p_2/p_1 = 10$.

h	$E_{h,\infty}(u_{1h})$	$E_{h,0}(u_{1h})$	$E_{h,1}(u_{1h})$	$E_{h,\infty}(u_{2h})$	$E_{h,0}(u_{2h})$	$E_{h,1}(u_{2h})$
1/8	1.893(−5)	6.676(−6)	3.499(−4)	1.893(−5)	6.543(−6)	3.431(−4)
1/16	2.593(−6)	9.540(−7)	9.912(−5)	2.593(−6)	9.409(−7)	9.795(−5)
1/32	3.289(−7)	1.192(−7)	2.474(−5)	3.289(−7)	1.175(−7)	2.440(−5)
1/64	4.141(−8)	1.490(−8)	6.182(−6)	4.141(−8)	1.469(−8)	6.094(−6)
1/128	5.195(−9)	1.867(−9)	1.551(−6)	5.195(−9)	1.841(−9)	1.529(−6)
1/256	6.537(−10)	2.347(−10)	3.895(−7)	6.531(−10)	2.314(−10)	3.841(−7)

Table 14
Errors in the IFE solutions $u_{ih},\ i = 1, 2$, generated in the quadratic IFE space $\widetilde{S}_h(\Omega)$ with $p_2/p_1 = 10^4$.

h	$E_{h,\infty}(u_{1h})$	$E_{h,0}(u_{1h})$	$E_{h,1}(u_{1h})$	$E_{h,\infty}(u_{2h})$	$E_{h,0}(u_{2h})$	$E_{h,1}(u_{2h})$
1/8	1.893(−5)	6.423(−6)	3.368(−4)	1.893(−5)	6.420(−6)	3.369(−4)
1/16	2.593(−6)	9.256(−7)	9.609(−5)	2.593(−6)	9.264(−7)	9.626(−5)
1/32	3.289(−7)	1.157(−7)	2.401(−5)	3.289(−7)	1.159(−7)	2.404(−5)
1/64	4.141(−8)	1.446(−8)	5.999(−6)	4.141(−8)	1.447(−8)	6.002(−6)
1/128	5.195(−9)	1.811(−9)	1.505(−6)	5.195(−9)	1.810(−9)	1.505(−6)
1/256	6.531(−10)	2.280(−10)	3.782(−7)	6.531(−10)	2.282(−10)	3.785(−7)

Table 15
Errors in $I_h u_i,\ i = 3, 4$, generated in the quadratic IFE space $\widetilde{S}_h^2(\Omega)$ with $p_2/p_1 = 10$.

h	$E_{h,\infty}(I_h u_3)$	$E_{h,0}(I_h u_3)$	$E_{h,1}(I_h u_3)$	$E_{h,\infty}(I_h u_4)$	$E_{h,0}(I_h u_4)$	$E_{h,1}(I_h u_4)$
1/8	4.991(−2)	1.510(−2)	7.972(−1)	7.402(−2)	2.224(−2)	1.174(0)
1/16	6.241(−3)	1.905(−3)	1.998(−1)	9.238(−3)	2.807(−3)	2.943(−1)
1/32	7.801(−4)	2.412(−4)	5.030(−2)	1.153(−3)	3.562(−4)	7.421(−2)
1/64	1.147(−4)	3.091(−5)	1.301(−2)	3.916(−4)	4.885(−5)	2.163(−2)
1/128	1.515(−5)	3.850(−6)	3.925(−3)	6.653(−5)	5.816(−6)	1.116(−2)
1/256	7.696(−6)	4.941(−7)	1.231(−3)	3.482(−5)	8.864(−7)	4.411(−3)

Table 16
Errors in $I_h u_i,\ i = 3, 4$, generated in the quadratic IFE space $\overline{S}_h^2(\Omega)$ with $p_2/p_1 = 10$.

h	$E_{h,\infty}(I_h u_3)$	$E_{h,0}(I_h u_3)$	$E_{h,1}(I_h u_3)$	$E_{h,\infty}(I_h u_4)$	$E_{h,0}(I_h u_4)$	$E_{h,1}(I_h u_4)$
1/8	4.991(−2)	1.508(−2)	7.971(−1)	7.402(−2)	2.224(−2)	1.174(0)
1/16	6.241(−3)	1.895(−3)	1.996(−1)	9.238(−3)	2.807(−3)	2.943(−1)
1/32	8.275(−4)	2.426(−4)	5.041(−2)	1.153(−3)	3.552(−4)	7.407(−2)
1/64	9.014(−4)	5.514(−5)	2.915(−2)	1.441(−4)	4.494(−5)	1.872(−2)
1/128	3.677(−5)	3.911(−6)	6.452(−3)	1.801(−5)	5.649(−6)	4.686(−3)
1/256	2.833(−5)	6.480(−7)	3.552(−3)	2.251(−6)	7.061(−7)	1.172(−3)

Table 17
Errors in $I_h u_i,\ i = 3, 4$, generated in the quadratic IFE space $\widehat{S}_h^2(\Omega)$ with $p_2/p_1 = 10$.

h	$E_{h,\infty}(I_h u_3)$	$E_{h,0}(I_h u_3)$	$E_{h,1}(I_h u_3)$	$E_{h,\infty}(I_h u_4)$	$E_{h,0}(I_h u_4)$	$E_{h,1}(I_h u_4)$
1/8	4.991(−2)	1.501(−2)	7.962(−1)	7.402(−2)	2.209(−2)	1.172(0)
1/16	6.241(−3)	1.892(−3)	1.994(−1)	9.238(−3)	2.786(−3)	2.935(−1)
1/32	7.801(−4)	2.396(−4)	5.009(−2)	1.153(−3)	3.528(−4)	7.375(−2)
1/64	9.752(−5)	3.039(−5)	1.262(−2)	1.441(−4)	4.474(−5)	1.858(−2)
1/128	1.219(−5)	3.837(−6)	3.183(−3)	1.801(−5)	5.649(−6)	4.686(−3)
1/256	1.524(−6)	4.796(−7)	7.958(−4)	2.251(−6)	7.061(−7)	1.171(−3)

Table 18
Errors in the IFE solutions $u_{ih},\ i = 3, 4$, generated in the quadratic IFE space $\widetilde{S}_h^2(\Omega)$ with $p_2/p_1 = 10$.

h	$E_{h,\infty}(u_{3h})$	$E_{h,0}(u_{3h})$	$E_{h,1}(u_{3h})$	$E_{h,\infty}(u_{4h})$	$E_{h,0}(u_{4h})$	$E_{h,1}(u_{4h})$
1/8	4.990(−2)	1.505(−2)	7.963(−1)	7.401(−2)	2.216(−2)	1.172(0)
1/16	6.241(−3)	1.897(−3)	1.994(−1)	9.233(−3)	2.796(−3)	2.936(−1)
1/32	7.802(−4)	2.402(−4)	5.012(−2)	1.154(−3)	3.547(−4)	7.388(−2)
1/64	9.761(−5)	3.055(−5)	1.269(−2)	2.200(−4)	4.630(−5)	1.926(−2)
1/128	1.220(−5)	3.854(−6)	3.570(−3)	3.541(−5)	5.860(−6)	8.569(−3)
1/256	3.507(−6)	4.943(−7)	9.597(−4)	1.583(−5)	8.887(−7)	2.699(−3)

Table 19
Errors in the IFE solutions $u_{ih},\ i = 3, 4$, generated in the quadratic IFE space $\overline{S}_h^2(\Omega)$ with $p_2/p_1 = 10$.

h	$E_{h,\infty}(u_{3h})$	$E_{h,0}(u_{3h})$	$E_{h,1}(u_{3h})$	$E_{h,\infty}(u_{4h})$	$E_{h,0}(u_{4h})$	$E_{h,1}(u_{4h})$
1/8	4.990(−2)	1.503(−2)	7.962(−1)	7.400(−2)	2.217(−2)	1.172(0)
1/16	6.241(−3)	1.887(−3)	1.994(−1)	9.233(−3)	2.796(−3)	2.936(−1)
1/32	7.813(−4)	2.430(−4)	5.115(−2)	1.153(−3)	3.538(−4)	7.383(−2)
1/64	6.143(−4)	4.837(−5)	2.463(−2)	1.442(−4)	4.481(−5)	1.864(−2)
1/128	3.307(−5)	3.893(−6)	6.221(−3)	1.801(−5)	5.649(−6)	4.686(−3)
1/256	2.430(−5)	6.157(−7)	3.370(−3)	2.251(−6)	7.061(−7)	1.172(−3)

Table 20
Errors in the IFE solutions $u_{ih},\ i = 3, 4$, generated in the quadratic IFE space $\widehat{S}_h^2(\Omega)$ with $p_2/p_1 = 10$.

h	$E_{h,\infty}(u_{3h})$	$E_{h,0}(u_{3h})$	$E_{h,1}(u_{3h})$	$E_{h,\infty}(u_{4h})$	$E_{h,0}(u_{4h})$	$E_{h,1}(u_{4h})$
1/8	4.990(−2)	1.499(−2)	7.962(−1)	7.400(−2)	2.207(−2)	1.172(0)
1/16	6.241(−3)	1.891(−3)	1.994(−1)	9.231(−3)	2.785(−3)	2.935(−1)
1/32	7.802(−4)	2.396(−4)	5.009(−2)	1.152(−3)	3.527(−4)	7.375(−2)
1/64	9.752(−5)	3.039(−5)	1.262(−2)	1.441(−4)	4.474(−5)	1.858(−2)
1/128	1.219(−5)	3.837(−6)	3.183(−3)	1.801(−5)	5.649(−6)	4.686(−3)
1/256	1.524(−6)	4.796(−7)	7.958(−4)	2.251(−6)	7.061(−7)	1.171(−3)

References

[1] I. Babuška, The finite element method for elliptic equations with discontinuous coefficients, Computing 5 (1970) 207–213.

[2] I. Babuška and J.E. Osborn, Generalized finite element methods: their performance and relation to mixed methods, SIAM J. Numer. Anal. 20(3) (1983) 510–536.

[3] I. Babuška and J.E. Osborn, Finite element methods for the solution of problems with rough input data, in: *Singular and Constructive Methods for their Treatment*, eds. P. Grisvard, W. Wendland and J.R. Whiteman, Lecture Notes in Math., Vol. 1121 (Springer, New York, 1985) pp. 1–18.

[4] D. Braess, *Finite Elements* (Cambridge University Press, 1997).

[5] J.H. Bramble and J.T. King, A finite element method for interface problems in domains with smooth boundary and interfaces, Preprint (1995).

[6] S.C. Brenner and L. Ridgeway Scott, *The Mathematical Theory of Finite Element Methods*, Texts in Appl. Math., Vol. 15 (Springer, New York, 1994).

[7] Z. Chen and J. Zou, Finite element methods and their convergence for elliptic and parabolic interface problems, Numer. Math. 79 (1998) 175–202.

[8] A. Dadone and B. Grossman, Progressive optimization of inverse fluid dynamic design problems, Comput. Fluids 29 (2000) 1–32.

[9] A. Dadone and B. Grossman, An immersed body methodology for inviscid flows on Cartesian grids, AIAA Paper 2002-1059 (2002).

[10] R. Ewing, Z. Li, T. Lin and Y. Lin, The immersed finite volume element method for the elliptic interface problems, Math. Comput. Simulation 50 (1999) 63–76.

[11] B. Heinrich, *Finite Difference Methods on Irregular Networks*, Internat. Ser. Numer. Math., Vol. 82 (Birkhäuser, Boston, 1987).

[12] D.W. Hewett, The embedded curved boundary method for orthogonal simulation meshes, J. Comput. Phys. 138 (1997) 585–616.

[13] C. Johnson, *Numerical Solution of Partial Differential Equations by the Finite Element Method* (Cambridge Univ. Press, Cambridge, 1987).

[14] R.J. LeVeque and Z. Li, The immersed interface method for elliptic equations with discontinuous coefficients and singular sources, SIAM J. Numer. Anal. 34 (1994) 1019–1044.

[15] Z. Li, The immersed interface method using a finite element formulation, Appl. Numer. Math. 27 (1998) 253–267.

[16] Z. Li, T. Lin, Y. Lin and R. Rogers, An immersed finite element space and its approximation capability, Numer. Methods Partial Differential Equations (2003).

[17] Z. Li, T. Lin and X. Wu, New cartesian grid methods for interface problems using finite element formulation, Numer. Math. 96 (2003) 61–98.

[18] T. Lin, Y. Lin, R.C. Rogers and L.M. Ryan, A rectangular immersed finite element method for interface problems, in: *Advances in Computation: Theory and Practice*, Vol. 7 (2001) pp. 107–114.

[19] T. Lin and J. Wang, An immersed finite element electric field solver for ion optics modeling, in: *Proceedings of AIAA Joint Propulsion Conference*, Indianapolis, IN, July 2002, AIAA Paper 2002-4263 (2002).

[20] C.S. Peskin, Numerical analysis of blood flow in the heart, J. Comput. Phys. 25 (1977) 220–252.

[21] C.S. Peskin, Lectures on Mathematical Aspects of Physiology, in: Lectures in Appl. Math., Vol. 19 (Amer. Math. Soc., Providence, RI, 1981) pp. 69–107.

[22] M.P. Robinson and G. Fairweather, Orthogonal spline collocation methods for Schrödinger-type equations in one space variable, Numer. Math. 68 (1994) 355–376.

[23] A.A. Samarskiĭ and V.B. Andreev, *Méthods aux différences pour équations elliptiques* (Mir, Moscow, 1978).

[24] S. Zhu, G. Yuan and W. Sun, Convergence and stability of explicit/implicit schemes for parabolic equations with discontinuous coefficients, Internat. J. Numer. Anal. Modelling (2004).